Shc1 cooperates with Frs2 and Shp2 to recruit Grb2 in FGF-induced lens development

Qian Wang[1, §], Hongge Li[1, §], Yingyu Mao[1, §], Ankur Garg[1], Eun Sil Park[1], Yihua Wu[1], Alyssa Chow[1], John Peregrin[1], Xin Zhang [1, 2*]

[1]Department of Ophthalmology, Columbia University, New York, NY 10032, USA

[2]Department of Pathology and Cell Biology, Columbia University, New York, NY, USA

[*]Author for correspondence (e-mail: xz2369@columbia.edu)

[§] These authors contributed equally to this work

Abstract

Fibroblast growth factor (FGF) signaling elicits multiple downstream pathways, most notably the Ras/MAPK cascade facilitated by the adaptor protein Grb2. However, the mechanism by which Grb2 is recruited to the FGF signaling complex remains unresolved. Here we showed that genetic ablation of FGF signaling prevented lens induction by disrupting transcriptional regulation and actin cytoskeletal arrangements, which could be reproduced by deleting the juxtamembrane region of the FGF receptor and rescued by Kras activation. Conversely, mutations affecting the Frs2-binding site on the FGF receptor or the deletion of Frs2 and Shp2 primarily impact later stages of lens vesicle development involving lens fiber cell differentiation. Our study further revealed that the loss of Grb2 abolished MAPK signaling, resulting in a profound arrest of lens development. However, disrupting the Grb2 binding site on Shp2 or abrogating Shp2 phosphatase activity only modestly influenced FGF signaling, whereas mutating the presumed Shp2 dephosphorylation site on Grb2 did not impede MAPK signaling in lens development, indicating that Shp2 is only partially responsible for Grb2 recruitment. In contrast, we observed that FGF signaling is required for the phosphorylation of the Grb2-binding sites on Shc1 and the deletion of Shc1 exacerbates the lens vesicle defect caused by Frs2 and Shp2 deletion. These results reveal that Shc1 collaborates with Frs2 and Shp2 to target Grb2 in FGF signaling.

Introduction

The lens is an exemplary model for studying signaling pathways (Cvekl and Zhang, 2017). In mice, the lens placode emerges as thickened epithelia within the lateral head ectoderm at E9.5 (Fig. 1A). It undergoes invagination to form the lens pit at E10.5, and upon separation from the surface ectoderm, progresses into the lens vesicle at E11.5. Following this, lens progenitor cells within the lens vesicle proliferate and migrate toward the equator of the lens, where they differentiate into lens fibers responsible for the lens's focusing power (Lovicu and McAvoy, 2005). Genetic modification of the FGF signaling cascade alters various lens developmental processes, including lens invagination (Carbe and Zhang, 2011; Pan et al., 2006), lens vesicle formation (Kuracha et al., 2011), the establishment of the transition zone (Li et al., 2019), lens epithelium proliferation and survival, as well as lens fiber differentiation and elongation (Lovicu and Overbeek, 1998; Qu et al., 2011b; Robinson et al., 1995; Zhao et al., 2008). Therefore, the lens provides valuable insights into the nuanced interplay of FGF signaling components during distinct stages of lens formation.

The current model of FGF signaling posits that its primary orchestration centers on the Frs2/Shp2/Grb2 complex (Beenken and Mohammadi, 2009; Brewer et al., 2016; Eswarakumar et al., 2005). According to this model, FGFR activation induces phosphorylation of the adaptor protein Frs2, creating a platform for recruiting Shp2 and Grb2. In conjunction with its constitutively bound partner Sos (a guanine nucleotide exchange factor), Grb2 subsequently initiates Ras/MAPK signaling (Hadari et al., 2001; Ong et al., 2000). Prior research in eye development supports this notion, revealing that Crk proteins augment Ras signaling by associating with the Frs2/Shp2/Grb2 complex (Collins et al., 2018; Li et al., 2014; Madakashira et al., 2012), while PI3K-AKT signaling is activated through direct Ras binding with the PI3K

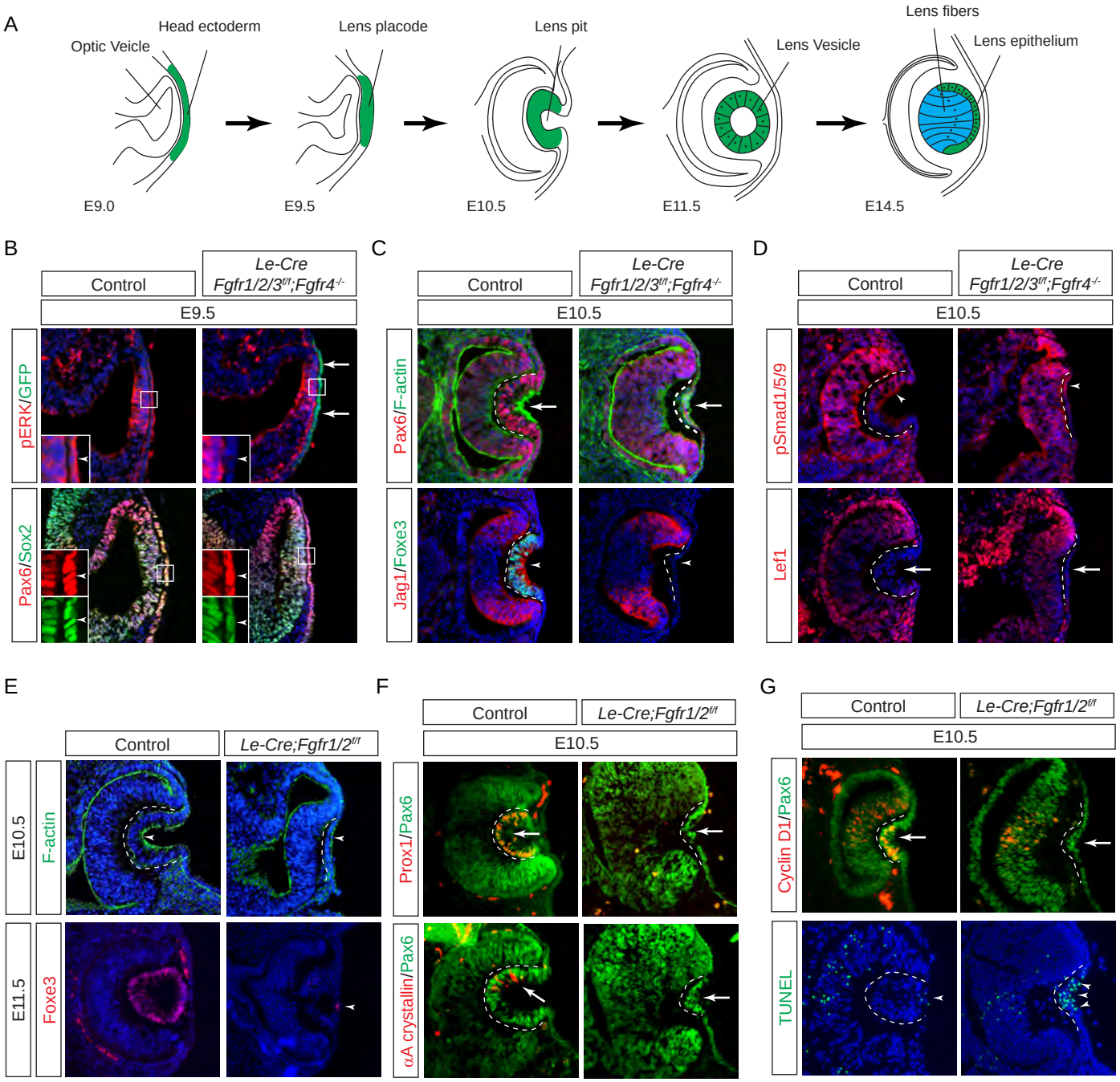

Figure 1. FGF Signaling Regulates Lens Development in a Dose-Dependent Manner. (A) Schematic diagram of murine lens development. The head ectoderm is induced by the underlying optic vesicle to become the lens placode, which subsequently folds inwards to become the lens pit. The closure of the lens vesicle sets the stage for the differentiation of the lens epithelium into the lens fibers. **(B)** Depletion of all four *Fgfr1/2/3/4*, driven by *Le-Cre* and traced with GFP, led to a thinner lens placode, evident from the absence of pERK signals and the failure to upregulate Sox2 like Pax6 (inserts, arrowheads). **(C)** *Fgfr1/2/3/4* mutants displayed disrupted apical constriction (F-actin accumulation, arrows) and lacked lens-specific expression of Foxe3 and Jag1 (arrowheads). Dotted lines outline the lens pit. **(D)** Despite *Fgfr1/2/3/4* mutations, BMP (pSmad1/5/9 staining, arrowheads) and Wnt signaling (Lef1 expression, arrows) remained unaffected. **(E)** The absence of *Fgfr1/2* alone did not impede the apical buildup of F-actin nor the expression of Foxe3, indicating partial retention of lens development processes. **(F)** Crucial lens markers, Prox1 and αA-crystallin, were absent in *Fgfr1/2* mutants, pointing to a significant developmental defect after the lens induction stage. **(G)** *Fgfr1/2* mutants exhibited loss of cell proliferation marker Cyclin D1 (arrows) and widespread apoptosis (TUNEL staining, arrowheads).

catalytic subunit p110 (Wang et al., 2021). However, unresolved questions persist regarding downstream mediators of FGF signaling. Earlier studies suggested that mice with Frs2 mutants lacking the Grb2 binding site can survive healthily, whereas those lacking the Shp2 binding site exhibit severe eye development defects and significantly reduced MAPK signaling (Gotoh et al., 2004). These results suggest the critical importance of Shp2 in Grb2-mediated Ras signaling, but the exact mechanism remains unclear. Additionally, Soriano and colleagues generated allelic series of *Fgfr1* and *Fgfr2* mutants disrupting the Frs2 binding sites and multiple tyrosine phosphorylation residues, both individually and in combination, yet their phenotypes proved less severe than those of the respective null mutants (Brewer et al., 2015; Clark and Soriano, 2024) These studies suggest that there may exist additional adaptor(s) other than Frs2 to mediate FGF signaling.

In this study, we demonstrated that genetic alterations to FGFR— whether by deleting all isoforms, the juxtamembrane region, or the specific Frs2 binding site—disrupt the successive phases of lens development, encompassing lens induction, vesicle formation, and fiber differentiation. Surprisingly, while we established that Grb2-Ras signaling serves as the primary conduit of FGF signaling, interfering with Grb2 dephosphorylation and binding by Shp2 or even abolishing Shp2 phosphatase activity did not eliminate either MAPK signaling or lens differentiation. Conversely, we observed that FGF-induced Shc phosphorylation hinges on the FGFR juxtamembrane domain rather than its Frs2 binding site. Although the deletion of Shc1 has only a modest impact on lens development and MAPK activity individually, its combination with Frs2 and Shp2 deletion results in a profound arrest of lens vesicle development. These results suggest that Shc functions independently of Frs2 and Shp2 to augment Grb2-Ras signaling within the FGF pathway.

Results

FGF signaling is required for lens induction.

Previous studies have established the presence of all four FGF receptors in the surface ectoderm during lens induction (Garcia et al., 2011). However, despite the deletion of the primary FGFRs, *Fgfr1* and *Fgfr2*, only thinning of the lens placode occurred, with no discernible impact on lens determination transcription factors like Pax6, Sox2, and Foxe3. To explore whether the compensatory effects of remaining FGFRs obscure the role of FGF signaling in lens induction, we eliminated all four FGFRs using the *Le-Cre* deletor driven by the *Pax6* lens ectoderm (LE) enhancer (Ashery-Padan et al., 2000). The *Le-Cre* activity within the lens placode at E9.5, as indicated by the embedded GFP reporter (Fig. 1B, arrows), resulted in the complete loss of pERK in the ectoderm, confirming FGF signaling inactivation (Fig. 1B, inserts and arrowheads). Consequently, while the initial marker of lens induction, increased Pax6 expression as the surface ectoderm transitions into the lens placode, persisted in the mutant, Sox2 expression remained at basal levels. Furthermore, subsequent lens placode invagination, driven by apical constriction evidenced by polarized F-actin localization on the apical side by E10.5 (Chauhan et al., 2011), was disrupted (Fig. 1C arrows). This occurred despite the proper localization of Fibronectin at the basal side of the lens placode (supplementary Fig. 1A), suggesting that overall cell polarity remained unaffected. The *Le-Cre;Fgfr1*$^{f/f}$*;Fgfr2*$^{f/f}$*;Fgfr3*$^{f/f}$*;Fgfr4*$^{-/-}$ mutant also failed to express lens-specific markers Foxe3 and Jag1, further underscoring impaired lens induction (Fig. 1C, arrowheads). Previous studies have highlighted FGF and BMP interaction during lens formation (Garcia *et al.*, 2011), yet the dorsal-to-ventral gradient of BMP signaling, as indicated

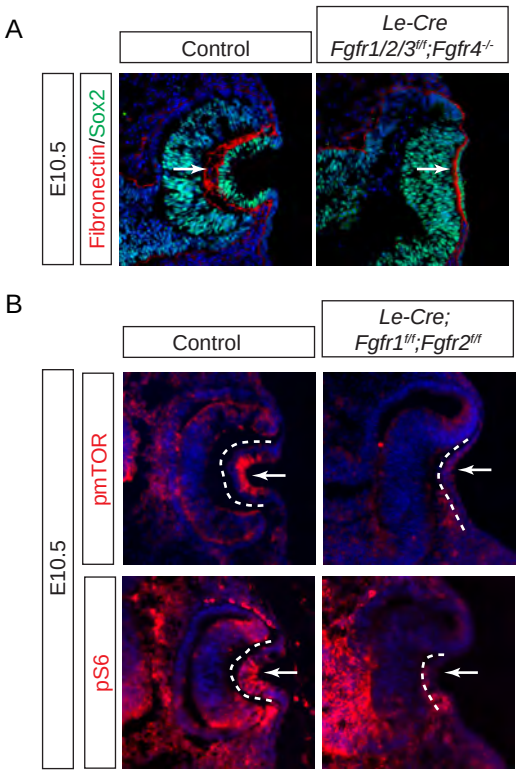

Supplementary Figure 1. Lens development in Fgf receptor mutants. (A) Depletion of all four *Fgfr1/2/3/4* did not disrupt the Fibronectin expression at the basal side of the lens placode (arrows). **(B)** pmTOR and pS6 staining were lost in *Le-Cre;Fgfr1*$^{f/f}$*;Fgfr2*$^{f/LR}$ lens.

by pSmad staining, persisted in *Le-Cre;Fgfr1*$^{f/f}$*;Fgfr2*$^{f/f}$*;Fgfr3*$^{f/f}$*;Fgfr4*$^{-/-}$ knockouts (Fig. 1D, arrowheads). Furthermore, Wnt signaling, a known negative regulator of lens induction (Smith et al., 2005), showed no signs of abnormal activity, as indicated by the absence of Lef1 expression (Fig. 1D, arrows). These results demonstrated that FGF signaling is required independently of Bmp and Wnt signaling for lens induction.

We next focused on the two primary FGFRs, Fgfr1 and 2, to scrutinize the latter phases of lens development. In contrast to mutants with deletion of all four FGFRs, we observed apical confinement of F-actin and expression of Foxe3 in the *Le-Cre;Fgfr1*$^{f/f}$*;Fgfr2*$^{f/f}$ mutant lens cells (Fig. 1E, arrows). However, there was a conspicuous reduction in phosphorylation of mTOR and its downstream target S6 in the lens vesicle, suggesting that deletion of *Fgfr1/2* disrupted mTOR signaling (Supplementary Fig. 1B, arrowheads). Underscoring the lens differentiation defect, Prox1, a crucial transcription factor for lens fiber development, along with the lens-specific protein αA crystallin expression, was also lost in the *Le-Cre;Fgfr1*$^{f/f}$*;Fgfr2*$^{f/f}$ mutant lens vesicle (Fig. 1F, arrows) (Garg et al., 2020; Ochi et al., 2003; Xie et al., 2016). Additionally, there was a notable decrease in Cyclin D1 expression and increasing TUNEL staining within the lens vesicle, indicating cell proliferation and apoptosis defects (Fig. 1G, arrows and arrowheads) (Garcia *et al.*, 2011).

Ras mediates FGF signaling to suppress apoptosis in the development lens.

FGF signaling is known to stimulate the Ras-MAPK signaling pathway. To explore the significance of Ras signaling, we employed a genetic rescue strategy utilizing an inducible *Kras* allele capable of expressing the constitutively active *Kras*^{G12D} upon Cre-mediated recombination (Fig. 2A) (Tuveson et al., 2004). When crossed with *Fgfr1/2* mutants, this allele effectively

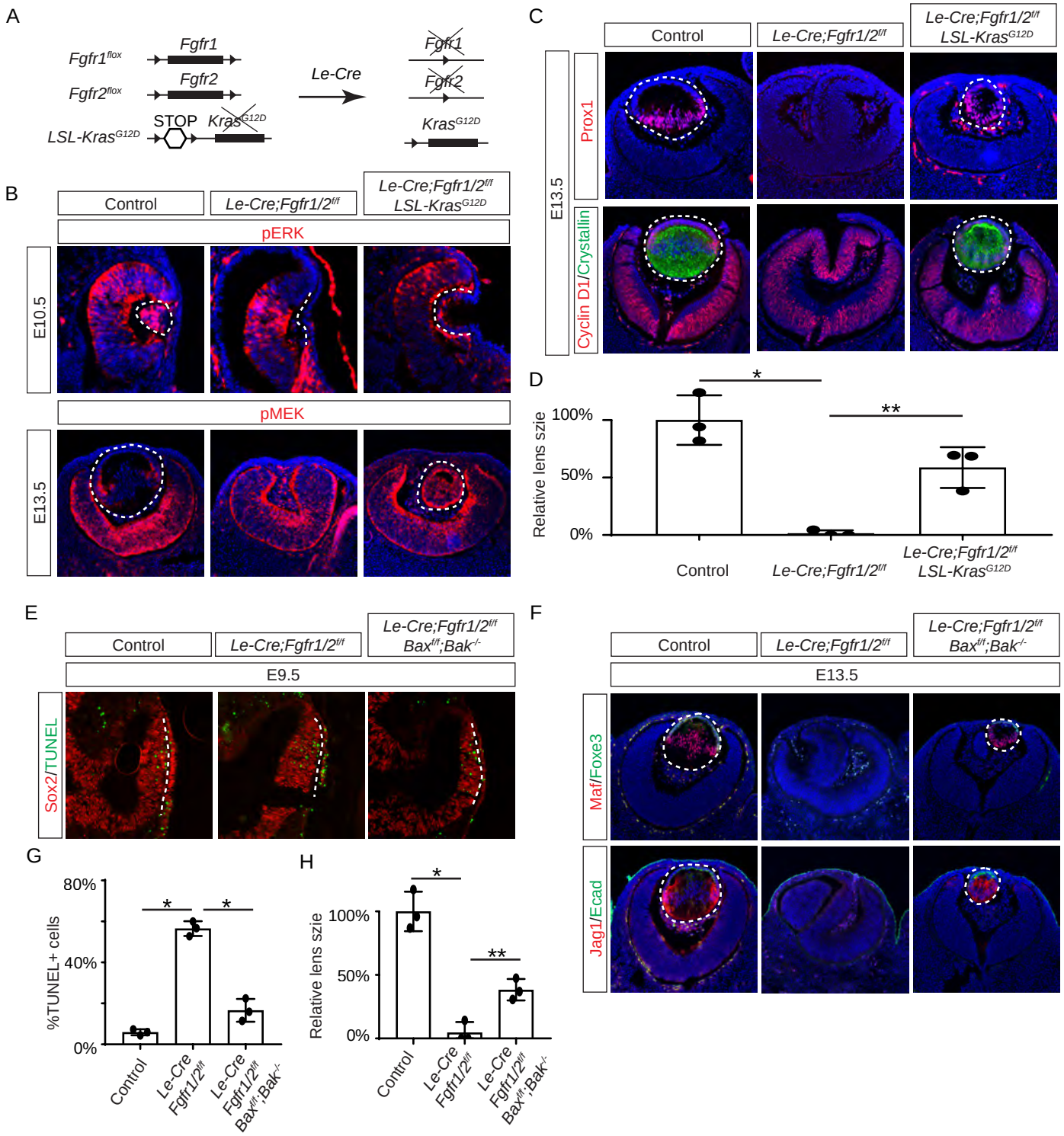

Figure 2. Restoration of Lens Development in FGF Signaling Mutants via Kras Activation and Apoptosis Inhibition. (A) The *Le-Cre* driver facilitated the excision of the floxed alleles of *Fgf1/2* along with the *LSL-STOP* cassette at the *Kras* locus, leading to the expression of the constitutively active *Kras*^{G12D} allele within the *Fgf1/2* mutant background. **(B)** The activation of Kras signaling in the FGF signaling mutant lenses reinstated pERK activity at E10.5 and pMEK expression at E13.5, indicating restoration of MAPK signaling. **(C)** The lens-specific expression of Prox1 and αA-crystallin were also recovered, indicating successful lens development rescue. **(D)** Quantification of the lens size. One way ANOVA, n=3, *P<0.001, **P<0.02. **(E)** The deletion of pro-apoptotic genes *Bak* and *Bax* in *Fgf1/2* mutants suppressed apoptosis as shown by TUNEL staining. **(F)** Inhibiting apoptosis in *Fgfr1/2* mutants facilitated lens formation, as indicated by the expression of lens differentiation markers Prox1, Maf, and Jag1. **(G)** Quantification cell apoptosis. One-way ANOVA, n=3, *P<0.001. **(G)** Quantification of the lens size. One-way ANOVA, n=3, *P<0.0001, **P<0.05.

restored pERK expression and normalized lens vesicle invagination (Fig. 2B). By E13.5, the *Le-Cre;Fgfr1*$^{f/f}$*;Fgfr2*$^{f/f}$*;Kras*^{G12D} lens displayed robust phosphorylation of MEK, the upstream kinase of Erk, concomitant with the expression of lens fiber markers Prox1 and αA crystallin (Fig. 2B and C). Notably, the rescued lens reached about half the size of a control lens (Fig. 2D). These results suggest that Kras signaling acts as a primary conduit for FGF signaling during lens development.

To ascertain whether cell death underpins the pronounced lens vesicle defect in *Le-Cre;Fgfr1*$^{f/f}$*;Fgfr2*$^{f/f}$ mutant, we targeted Bax and Bak, two core regulators of the intrinsic pathway of apoptosis, for deletion. This intervention notably reduced TUNEL signals within the lens placode (Fig. 2E and F) and resulted in a recovery of lens formation, as evidenced by the expression of Foxe3, Maf, and Jag1 (Fig. 2G), although the lens remained considerably smaller than the wild-type control (Fig. 2H). This underscores the critical role of FGF signaling in preventing excessive cell apoptosis during lens development.

The juxtamembrane domain and Frs2 binding site of FGFR regulate the consecutive steps of lens development.

Previous studies have mapped the Frs2 binding site to the juxtamembrane domain of FGFR (Dhalluin et al., 2000; Ong *et al.*, 2000). To probe the role of this region in lens development, we employed two distinct alleles: one entirely devoid of the juxtamembrane domain (amino acid 407-433 in Fgfr1, *Fgfr1*$^{\Delta Frs}$) (Hoch and Soriano, 2006), and another harboring mutations in two pivotal residues essential for Frs2 binding (L424A and R426A in Fgfr2, *Fgfr2*^{LR}) (Fig. 3A) (Eswarakumar et al., 2006). Intriguingly, while the *Fgfr1/2* compound mutant carrying *Fgfr1*$^{\Delta Frs}$ mirrored the null phenotype (Fig. 3B, arrowheads), the mutant featuring *Fgfr2*^{LR} exhibited

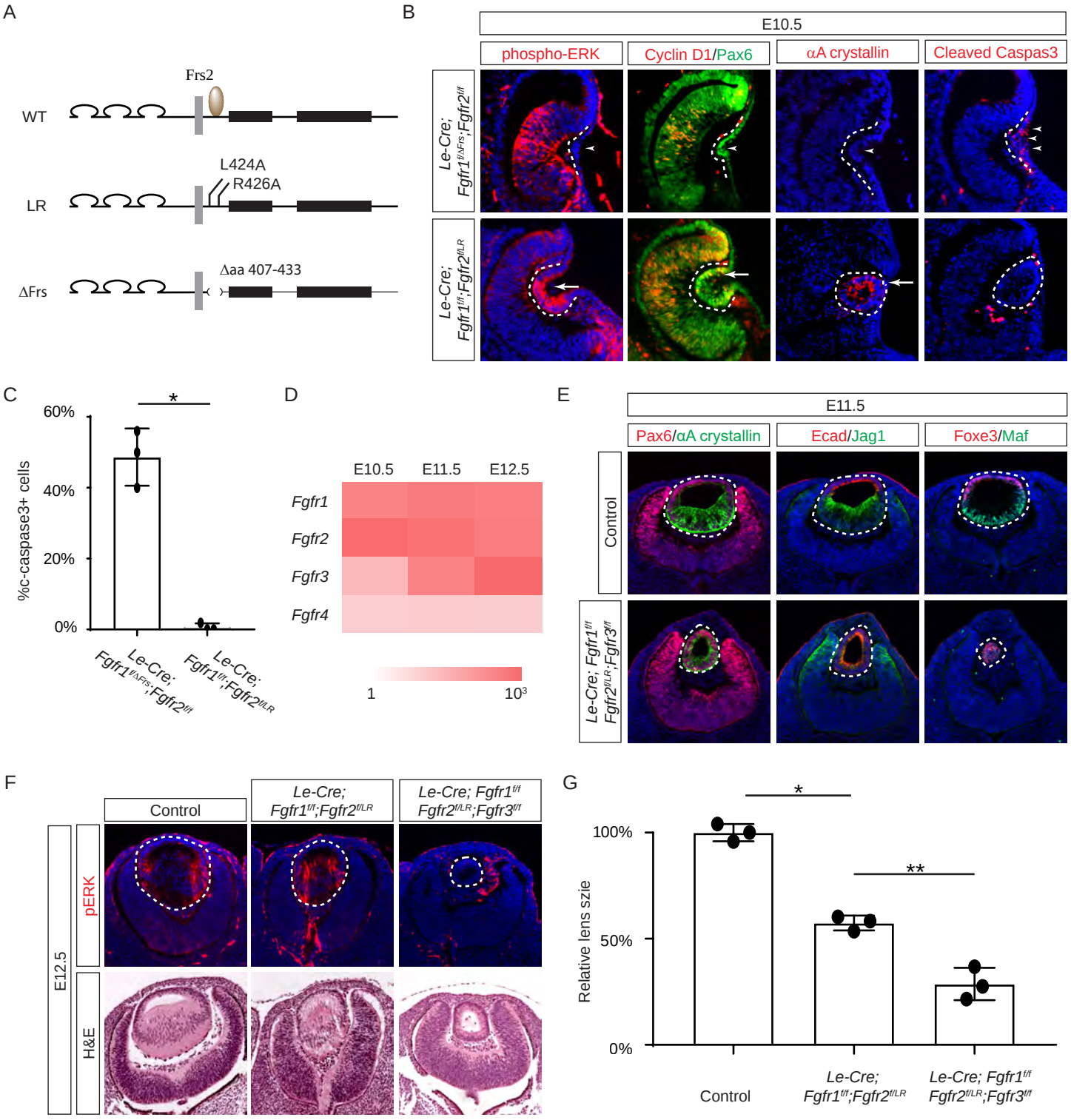

Figure 3. The Frs2 binding site on FGFR is only required for lens vesicle differentiation. **(A)** Overview of *Fgfr* mutant alleles. *Fgfr1*$^{\Delta Frs}$ lacks the Frs2 binding domain (amino acid 407-433), and *Fgfr2*^{LR} has point mutations disrupting Frs2 binding (L424A and L426A). **(B)** In *Fgf1/2* compound mutants, loss of pERK , CyclinD1, αA-crystallin and increased cleaved caspase3 were observed with the *Fgfr1*$^{\Delta Frs}$ allele but not the *Fgfr2*^{LR} allele. **(C)** Quantification of cleaved caspase3 staining. Student's t-test, n=3, *P<0.001. **(D)** Heatmap depicts Fgfr expression levels during lens development. **(E)** *Fgfr2*^{LR} mutants in the *Fgfr1/2/3* genetic background showed impaired lens vesicle differentiation, with posterior lens epithelial cells failing to elongate and activate lens fiber cell markers Jag1 and Maf. **(F)** *Fgfr1/2/3* triple mutants with *Fgfr2*^{LR} lost pERK staining and displayed a shallow lens vesicle at E12.5. **(G)** Quantification of the lens size. One-way ANOVA n=3, *P<0.001, **P<0.05.

sustained expression of pERK, Cyclin D1, and αA crystallin, with no discernible increase in cell death, as confirmed by cleaved caspase 3 staining (see Fig. 3B and C). This suggests that the juxtamembrane domain of FGFR likely serves additional functions beyond Frs2 binding in lens induction.

The absence of a lens induction phenotype in the *Le-Cre;Fgfr1*$^{f/f}$*;Fgfr2*$^{f/LR}$ mutant raised the question regarding the role of Frs2 in lens development. Upon examining the iSyTE lens gene expression database (Kakrana et al., 2018), we observed a rapid increase in *Fgfr3* expression in the murine lens from E11.5 onwards, surpassing the levels of both *Fgfr1* and *Fgfr2* by E12.5 (Fig. 3D). This led us to consider whether heightened *Fgfr3* expression could potentially mask the effects of *Fgfr2*^{LR} mutation during later stages of lens development. To explore this hypothesis, we further deleted *Fgfr3* in conjunction with the *Fgfr1* and *Fgfr2*^{LR} mutant, which indeed impeded the differentiation and elongation of posterior lens epithelial cells, as evidenced by the absence of αA crystallin, Jag1, and Maf at E11.5 (Fig. 3E). By E12.5, unlike the *Le-Cre;Fgfr1*$^{f/f}$*;Fgfr2*$^{f/LR}$ mutant, which retained pERK staining and generated lens fibers to populate the lens vesicle similar to controls, the *Le-Cre;Fgfr1*$^{f/f}$*;Fgfr2*$^{f/LR}$*;Fgfr3*$^{f/f}$ triple mutant remained a hollow lens vesicle without any pERK expression (Fig. 3F and G). This observation bears a striking resemblance to the phenotype previously reported when all three FGFRs were deleted at this stage (Zhao *et al.*, 2008). Thus, while the Frs2 binding site on FGFR is dispensable for lens induction and lens vesicle formation, it evidently emerges as crucial for the later stage of lens fiber differentiation.

Grb2 mediates FGF-MAPK signaling in lens cell differentiation.

If Frs2 is responsible for lens fiber differentiation rather than lens induction, we anticipate that its downstream target, Grb2, would exhibit a similar phenotype. To test this hypothesis, we genetically deleted *Grb2* using the *Le-Cre* driver. Indeed, the *Le-cre;Grb2*$^{f/f}$ mutant formed a lens vesicle at E12.5 but lacked pERK staining, correlating with decreased Cyclin D3 expression and increased TUNEL staining (Fig. 4A). Notably, the initial lens determination gene Foxe3 was unaffected, but differentiation marker Jag1 was absent while Maf and crystallin were reduced. This lens differentiation defect is evident as early as E11.5, characterized by a significant reduction in the expression of cell cycle regulators Cyclin D1 and p57, as well as the pro-differentiation transcription factor Prox1, suggesting dysregulation of the cell cycle and failure to initiate the lens fiber cell differentiation program (Fig. 4B). By E13.5, the lens vesicle remained hollow and smaller compared to the control (Fig. 4B and C). The deletion of Grb2 affects lens differentiation without hindering the formation of the lens vesicle, mirroring the effect of Frs2 binding site mutation, thus supporting the notion that Grb2 is the primary downstream effector of Frs2 in promoting lens fiber differentiation.

The Grb-Shp2 binding plays a modest role in FGF signaling.

While both Frs2 and Shp2 possess phosphotyrosine residues that can engage with Grb2 (Fig. 5A), it's noteworthy that only mutations in the Shp2 binding sites, rather than those in the Grb2 binding sites on Frs2, led to severe eye development defects (Gotoh *et al.*, 2004). This intriguing observation spurred us to investigate the potential role of Shp2 as an adaptor in facilitating the interaction between Frs2 and Grb2. To this end, we engineered a mouse model with mutations in the Grb2 binding sites of Shp2 (Sun et al., 2013) by substituting the C-terminal tyrosine residues

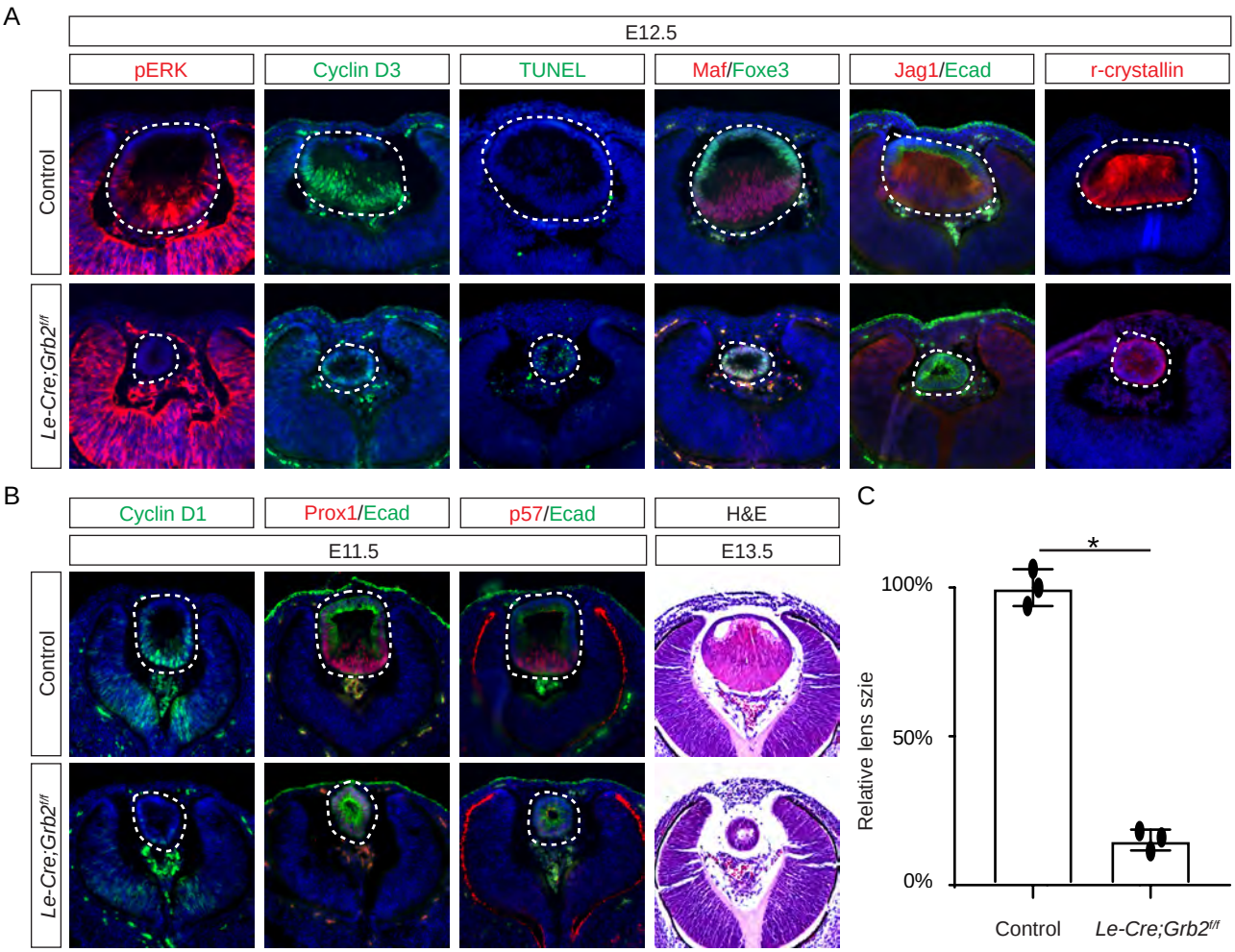

Figure 4. Grb2 is essential for lens vesicle survival, proliferation, and differentiation. (A) The targeted removal of Grb2 in the lens led to a loss of pERK signaling, reduced CyclinD3 expression, increased apoptosis (TUNEL staining), and disrupted expression of critical lens development genes Maf, Foxe3, Jag1 and γ-crystallin expression at E12.5. **(B)** Grb2 mutants Grb2 mutants displayed absent CyclinD1, Prox1, and p57 expression at E11.5 and remained an undifferentiated hollow vesicle at E13.5, failing to undergo normal lens fiber elongation. **(C)** Quantification of the lens size. Student's t-test, n=3, *P<0.0001.

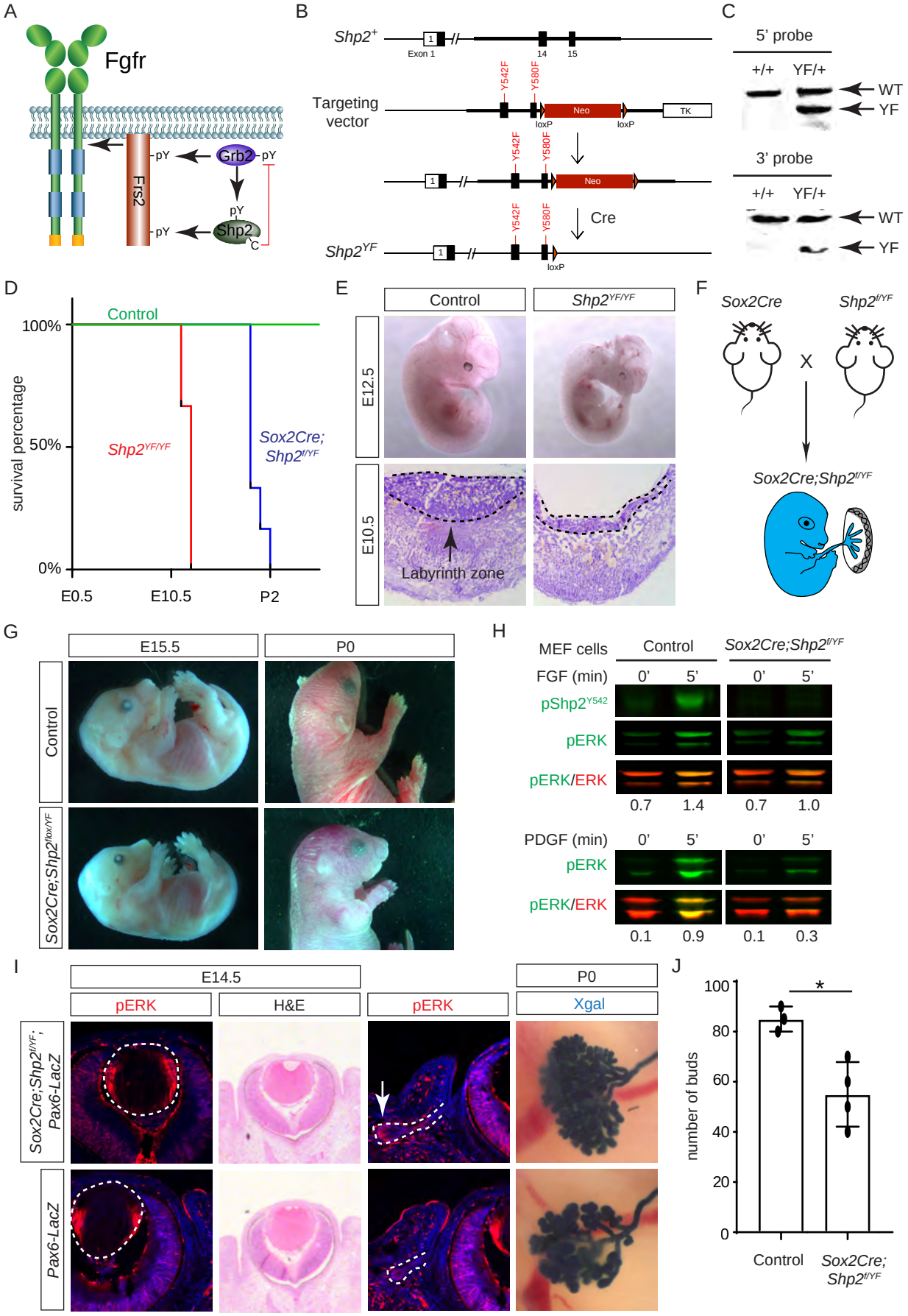

Figure 5. Shp2 C-terminal tyrosine phosphorylation is required for embryonic survival but dispensable for lens development. (A) Schematic of the core FGF signaling pathway. FGFR activation leads to phosphorylation of the adaptor Frs2 on N- and C-terminal tyrosines, recruiting Grb2 and Shp2 respectively. Shp2 can also bind Grb2 via its own C-terminal phosphotyrosines, and dephosphorylates Grb2 via its catalytic cysteine residue. **(B)** Generation of the *Shp2*^{YF} allele by homologous recombination to introduce *loxP*-flanked Neo and point mutations (Y542F and Y580F) disrupting the Shp2 C-terminal phosphotyrosine sites. The Neo cassette was subsequently excised by Cre-mediated recombination. **(C)** Validation of the *Shp2*^{YF} allele targeting was confirmed through Southern blot analysis with both 5' and 3' probes. **(D)** Kaplan-Meier survival curves demonstrate early lethality of *Shp2*^{YF} embryos (E12.5) and perinatal lethality of *Sox2Cre;Shp2*$^{f/YF}$ mutants. n=5 for *Shp2*$^{YF/YF}$ and n=6 for *Sox2Cre;Shp2*$^{f/YF}$ mutants. **(E)** *Shp2*$^{YF/YF}$ embryos displayed reduced body size at E12.5 and thinner labyrinth zones in their placenta E10.5. **(F)** *Sox2Cre*-mediated targeting restricts Shp2 deficiency to the embryonic proper, circumventing placental abnormalities. **(G)** *Sox2Cre;Shp2*$^{f/YF}$ mutants appeared grossly normal at E15.5 but failed to survive after birth. **(H)** While Y542 phosphorylation in Shp2 was lost as expected, *Sox2Cre;Shp2*$^{f/YF}$ MEFs exhibited a more pronounced reduction in pERK response to PDGF stimulation compared to FGF stimulation. **(I)** *Sox2Cre;Shp2*$^{f/YF}$ mutant lens displayed normal pERK staining and morphology, but reduced pERK in lacrimal glands at E14.5 and decreased bud numbers at P0. **(J)** Quantification of the number of lacrimal gland buds. Student's t-test, n=3, *P<0.02.

542 and 580 with phenylalanine (*Shp2*^{YF}) (Fig. 5B), which was confirmed by southern blot analysis using both 5' and 3' probes and Sanger sequencing (Fig. 5C). However, homozygous mice carrying the *Shp2*^{YF} mutation died around E12.5 with visibly paler and smaller bodies (Fig. 5D and E). Histological analysis of mutants revealed a significantly thinner labyrinth zone in placentas, crucial for oxygen and nutrient supplies (Fig. 5E, dotted lines). To test whether this placental defect is responsible for the embryonic lethality, we combined the *Shp2*^{YF} mutation with the *Shp2* conditional allele using *Sox2Cre*, which is specifically active in the epiblast-derived embryonic tissues but not in the trophoblast-derived placenta (Fig. 5F)(Hayashi and McMahon, 2002). *Sox2Cre;Shp2*$^{f/YF}$ embryos indeed survived past embryonic day 15.5 without evident morphological abnormalities, yet they succumbed shortly after birth for reasons yet unknown (Fig. 5G).

The survival of *Sox2Cre;Shp2*$^{f/YF}$ mutant beyond embryonic development permitted the isolation of mouse embryonic fibroblast (MEF) cells for biochemical analysis. As anticipated, the phosphorylation of Shp2 (pShp2^{Y542}) induced by FGF was abolished in *Sox2Cre;Shp2*$^{f/YF}$ MEF cells, yet the activation of pERK was only partially impaired (Fig. 5H). This contrasts with the more pronounced reduction in PDGF-induced ERK phosphorylation, underscoring a distinct requirement for Shp2-Grb2 binding across related receptor tyrosine kinase (RTK) pathways (Araki et al., 2003). In line with the subtle impact on FGF signaling, neither the pattern of pERK staining nor the size of the lens showed discernible alterations in *Sox2Cre;Shp2*$^{f/YF}$ mutants (Fig. 5I, arrowheads). We further investigated lacrimal gland development due to its remarkable sensitivity to FGF signaling intensity, where even a heterozygous *Fgf10* mutation has been shown to stunt gland growth (Garg and Zhang, 2017; Qu et al., 2011a). Notably, we observed a slight reduction in pERK staining in the lacrimal gland primordia at E14.5 and fewer lacrimal

gland buds at birth (Fig. 5I, arrows). These nuanced ocular phenotypes, alongside the overall normal morphology of *Sox2Cre;Shp2*$^{f/YF}$ mutant embryos, collectively suggest that Shp2-Grb2 binding exerts a modest influence on FGF signaling.

Inactivation of Shp2 phosphatase activity failed to abrogate FGF-induced MAPK signaling.

The results presented above indicate that the direct binding of Grb2 to the Shp2 C-terminus is not essential for FGF signaling. This led us to explore an alternative hypothesis that Shp2 might function by removing inhibitory tyrosine phosphorylation on Grb2, thereby promoting its interaction with Sos and subsequent Ras-MAPK activation (Ahmed et al., 2013; Vemulapalli et al., 2021). Based on the PhosphoSitePlus database, we identified Y209 as the most frequently phosphorylated tyrosine residue in Grb2 (Fig. 6A). Notably, previous studies have demonstrated that Shp2 dephosphorylates this specific site upon stimulation by various receptor tyrosine kinases (RTKs) (Ahmed *et al.*, 2013; Haines et al., 2009; Li et al., 2001; Riera et al., 2010). To assess the functional significance of Y209 phosphorylation, we generated a mutant *Grb2* allele where Y209 was replaced with phenylalanine (*Grb2*^{YF}) using the ES cell-based gene targeting technique (Fig. 6B and C). Surprisingly, our findings revealed that *Grb2*$^{YF/YF}$ homozygous mutants exhibited normal viability and fertility without any obvious phenotype. Additionally, the intensity of pERK staining in mutant lenses remained unchanged in mutant lenses compared to controls, and markers of the cell cycle (Ki67 and p57) as well as differentiation (Jag1, Foxe3, and Maf) were unaffected. These results suggest that despite being a frequent target for phosphorylation, Y209 on Grb2 is dispensable for FGF signaling.

The PhosphoSitePlus database indicates that Grb2 still possesses a less frequently phosphorylated Y160 site, which has also been previously implicated in FGF signaling (Ahmed

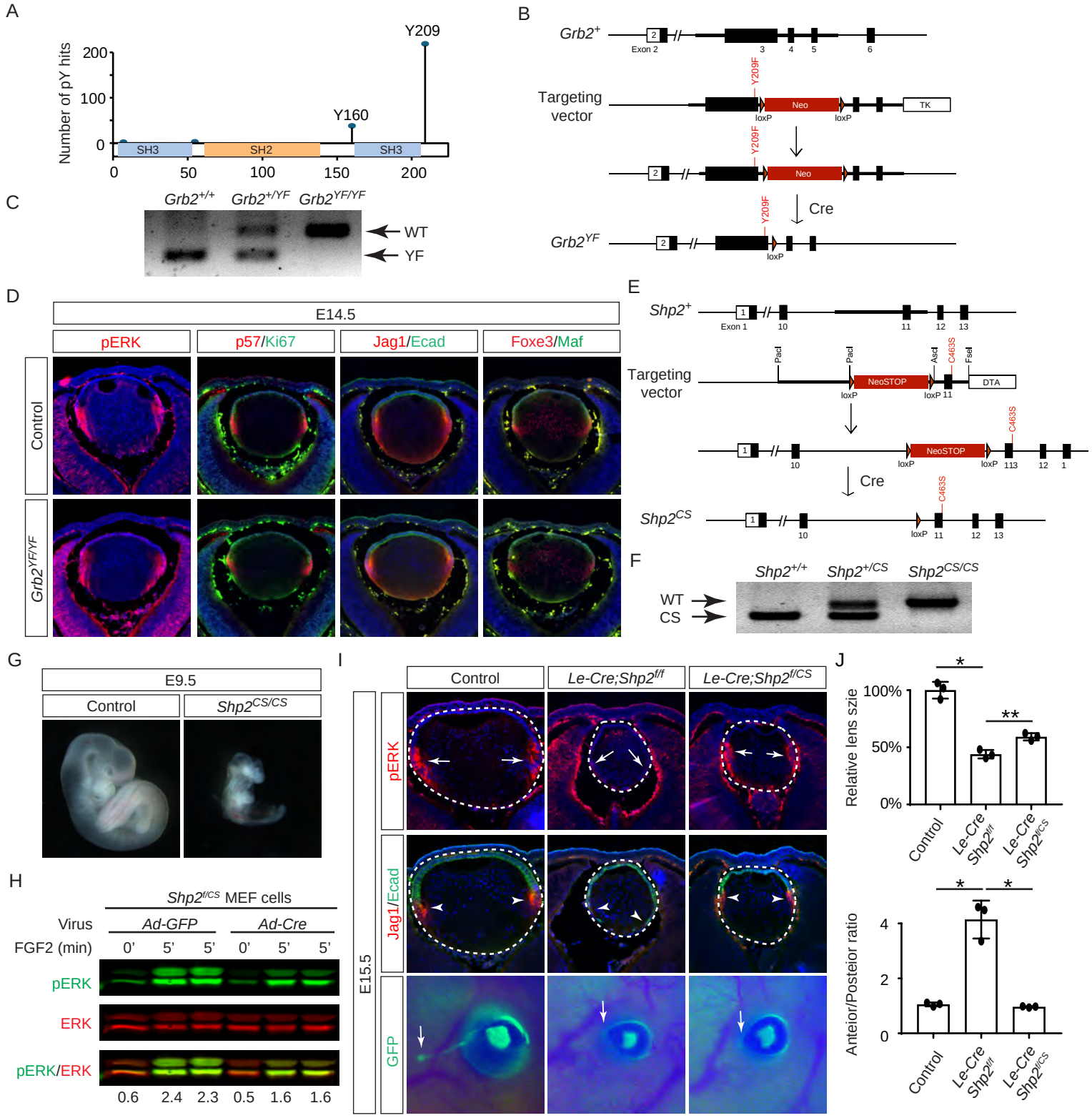

Figure 6. Shp2 phosphatase activity is partially required for FGF signaling independently of Grb2 dephosphorylation. **(A)** PhosphositePlus database indicates that Grb2 predominantly undergoes phosphorylation at Y209 and less frequently at Y160. **(B)** The *Grb2*^{YF} allele was constructed by homologous recombination to integrate a *loxP*-flanked *Neo* cassette and a Y209F point mutation into the *Grb2* locus. **(C)** PCR genotyping confirmed the presence of the *Grb2*^{YF} allele. **(D)** *Grb2* mutant lens typical expression patterns of pERK, cell cycle markers p57 and Ki67 and differentiation markers Foxe3, Maf and Jag1. **(E)** The *Shp2*^{CS} allele was generated by inserting the C459S mutation into the Shp2 locus by homologous recombination, followed by Cre-mediated removal of the *loxP*-flanked *Neo* cassette. **(F)** *Shp2*^{CS} allele validated by PCR genotyping. **(G)** *Shp2*$^{CS/CS}$ mutants exhibited growth retardation and died at E9.5. **(H)** *Shp2*$^{f/CS}$ MEF cells retained a significant capacity to activate pERK upon FGF stimulation after Cre virus infection. **(I)** *Le-Cre;Shp2*$^{f/f}$ mutants exhibited loss of pERK and Jag1 staining at the lens transition zone (arrowheads), which also shifted posteriorly. *Le-Cre;Shp2*$^{f/CS}$ mutant lens, in contrast, maintained staining at the equatorial region. Notably, both mutant types lacked lacrimal gland buds (arrows). **(J)** Quantification of the lens size. One-way ANOVA n=3, *P<0.0001, **P<0.001. **(K)** Quantification of the lens perimeter spanning the anterior epithelium versus that of the posterior lens fiber. One-way ANOVA n=3, *P<0.001.

et al., 2015). To rigorously assess the potential impact of Shp2-mediated Grb2 dephosphorylation, we developed a *Shp2*^{CS} mouse model by substituting the cysteine residue at position 463 (C459 in humans) with alanine in Shp2's catalytic domain, effectively abolishing its enzymatic activity (Fig. 6E and F). Unlike the earlier *Shp2* null mutants that perished by E7.5 (Yang et al., 2006), *Shp2*$^{CS/CS}$ embryos exhibited stunted growth but survived until E9.5, indicating that the *Shp2*^{CS} mutation doesn't entirely abrogate Shp2's function (Fig. 6G). Moreover, after removing the *flox* allele using Cre-expressing adenovirus, the *Shp2*$^{f/CS}$ MEF cells still retained considerable pERK activity in response to FGF stimulation (Fig. 6H). This was mirrored in vivo, with pERK detection in the *Le-Cre;Shp2*$^{f/CS}$ lens but not in the *Le-Cre;Shp2*$^{f/f}$ mutants (Fig. 6I). Consequently, lens epithelial cells in *Le-Cre;Shp2*$^{f/f}$ mutants migrated to the posterior pole with reduced p57 and Jag1 expression, indicating impaired differentiation, but *Le-Cre;Shp2*$^{f/CS}$ lens epithelial cells showed proper p57-mediated cell cycle exit at the lens equator and initiated timely expression of Jag1 (Fig. 6J). However, these lenses showed normal proliferation (Ki67) but increased cell death (TUNEL), resulting in a smaller size (Supplementary Fig. 2). Moreover, the development of the FGF signaling-sensitive lacrimal gland was blocked in both *Le-Cre;Shp2*$^{f/f}$ and *Le-Cre;Shp2*$^{f/CS}$ mutants, a more pronounced effect than the modest reduction in lacrimal gland buds observed in *Shp2*$^{YF/YF}$ mutants (Fig. 6I). This suggests that inhibiting Shp2's phosphatase activity more significantly affects FGF signaling compared to obstructing its adaptor function, yet doesn't completely abolish FGF signaling.

Shc1 cooperates with Frs2 and Shp2 to promote lens development

The mild lens defects observed in *Shp2* mutants lacking either adaptor or phosphatase function led us to investigate alternative mechanisms for Grb2 recruitment to the FGFR complex. Given the distinct lens phenotypes in *Le-Cre;Fgfr1*$^{f/f}$*;Fgfr2*$^{f/LR}$ and *Le-Cre;Fgfr1*$^{f/\Delta Frs}$*;Fgfr2*$^{f/f}$

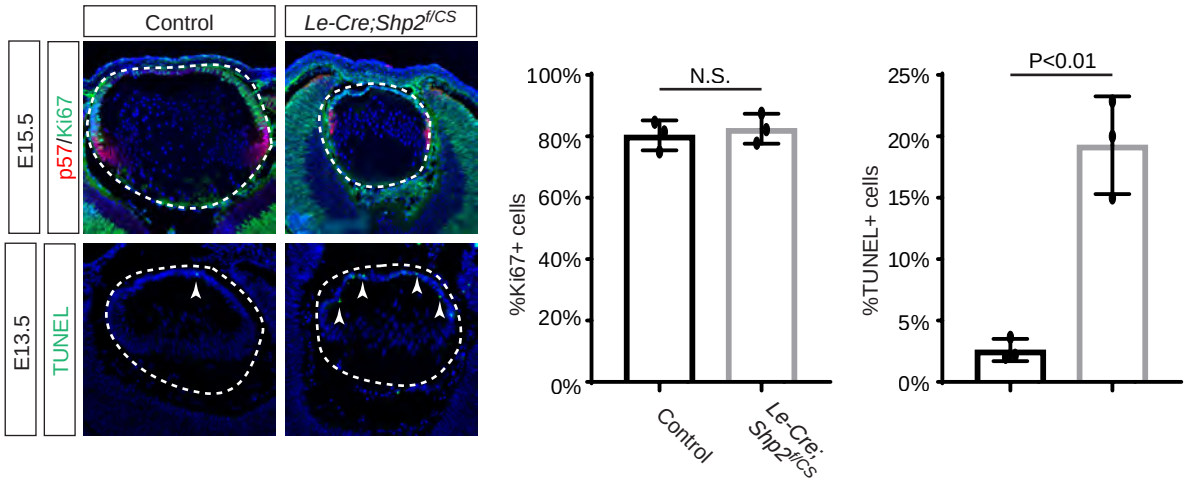

Supplementary Figure 2. Cell proliferation and apoptosis in *Shp2*^{CS} mutants. *Le-Cre;Shp2*$^{f/CS}$ lens exhibits normal expression of proliferation marker Ki67, but there is a significant increase in TUNLE+ cells (arrowheads). Student's t-test, N.S. (not significant) for %Ki67+ cells and P<0.01 for %TUNEL+ cells in the lens epithelium.

mutants (Fig. 7A), we hypothesized that FGF might activate unidentified factor(s) in *Fgfr1*$^{f/f}$*;Fgfr2*$^{f/LR}$ MEF cells but not in *Fgfr1*$^{f/\Delta Frs}$*;Fgfr2*$^{f/f}$ cells following the excision of flox alleles by Cre-expressing adenovirus, mirroring the observed pattern of pERK activation. Interestingly, FGF stimulation was ineffective in raising pFrs2 and pShp2 levels in both sets of MEF cells and did not alter the phosphorylation states of Crk and Gab1, both recognized adaptors in FGF signaling (Collins *et al.*, 2018; Hadari *et al.*, 2001; Li *et al.*, 2014). However, a key difference emerged – Shc phosphorylation was lost in *Fgfr1*$^{f/\Delta Frs}$*;Fgfr2*$^{f/f}$ cells but persisted in *Fgfr1*$^{f/f}$*;Fgfr2*$^{f/LR}$ mutants (Fig. 7A). This observation was further supported by in vivo data, which showed that pShc was detectable in both wild-type and *Le-Cre;Fgfr1*$^{f/f}$*;Fgfr2*$^{f/LR}$ lens vesicles, but not in *Le-Cre;Fgfr1*$^{f/\Delta Frs}$*;Fgfr2*$^{f/f}$ mutants (Fig. 7B, arrowhead). These findings suggest that Shc can be activated by the FGFR independently of its Frs2 binding site, potentially serving as an alternate route for Grb2's engagement.

Among the four *Shc* genes present in the mammalian genome, *Shc1* is the most abundant in the lens (Fig. 7C). This led us to ablate *Shc1* in the lens to determine its function in FGF signaling. However, *Le-Cre;Shc1*$^{f/f}$ lenses displayed only minor reductions in pERK staining and size, suggesting potential redundancy with other Shc proteins or compensatory mechanisms involving Frs2 and Shp2. To investigate this further, we created compound mutants involving these genes. We have previously reported that the deletion of *Frs2* or *Shp2* alone led to a modest diminution in lens size, akin to the *Shc1* deletion effect. However, the combined knockout of *Frs2* and *Shp2* (*Le-Cre;Frs2*$^{f/f}$*;Shp2*$^{f/f}$) resulted in hollow lens vesicles, highlighting a synergistic interaction between these two genes (Li *et al.*, 2014). While the *Le-Cre;Frs2*$^{f/f}$*;Shc1*$^{f/f}$ compound mutant did not exhibit as severe abnormalities, introducing the *Shc1* knockout into the *Le-Cre;Frs2*$^{f/f}$*;Shp2*$^{f/f}$ background further diminished the lens size, suggesting that Shc1 contributes

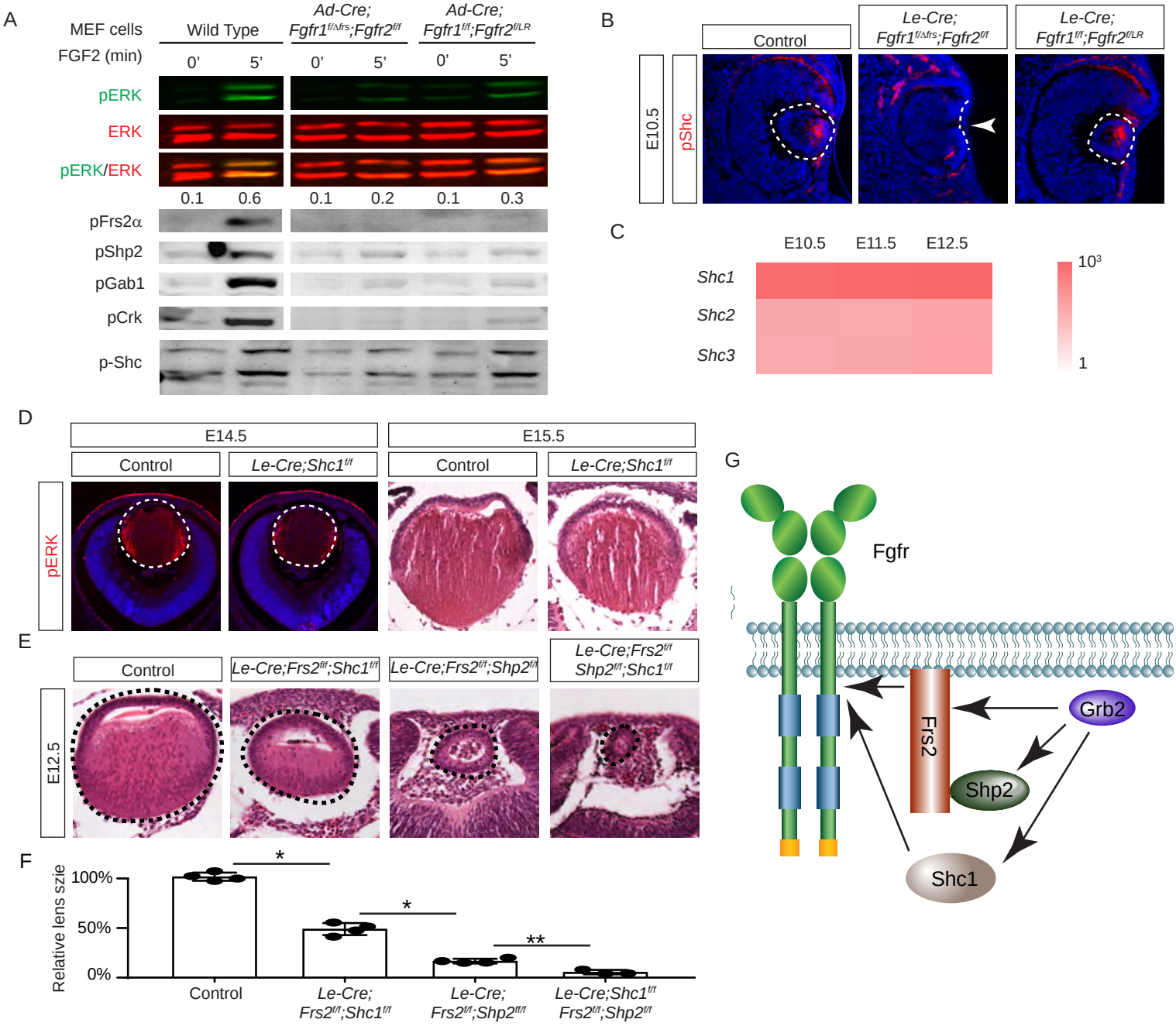

Figure 7. Shc1 complements Frs2 and Shp2 in mediating FGF signaling in lens development. (A) *Fgfr1*$^{f/f}$*;Fgfr2*$^{f/LR}$ infected with Cre virus showed stronger pERK and pShc activation than *Fgfr1* $^{f/\Delta Frs}$*;Fgfr2*$^{f/f}$ MEF cells, despite both losing Frs2, Shp2, Gab1, and Crk phosphorylation. **(B)** pShc staining was lost in *Le-Cre;Fgfr1* $^{f/\Delta Frs}$*;Fgfr2*$^{f/f}$ mutant lens (arrowhead) but preserved in *Le-Cre;Fgfr1*$^{f/f}$*;Fgfr2*$^{f/LR}$ lens. **(C)** Heatmap showing Shc expression levels during lens development. **(D)** *Shc1*-deficient lenses showed a slight decrease in both pERK staining intensity and overall lens size. **(E)** E12.5 Frs2/Shc1 mutant lenses were smaller than controls, while lenses from Frs2/Shp2 mutants showed a pronounced hollow vesicle structure, a condition that worsened in Frs2/Shp2/Shc1 triple mutants. **(F)** Quantification of the lens size. One-way ANOVA n=4, *P<0.001, **P<0.05. **(G)** Model of FGF signaling network. Frs2 recruits Grb2 directly and indirectly through Shp2, while Shc1 provides an alternate Grb2 recruitment route independent of Frs2.

an additive role alongside Frs2 and Shp2 in modulating lens development. These findings collectively showed that Shc1 functions independently of Frs2 and Shp2 to transmit FGF signaling in lens development.

Discussion

This study used lens development as a model system to dissect the intricate mechanisms of FGF signaling. By systematically disrupting FGF signaling components, it unveiled a previously unappreciated dependency on precise FGF dosage for each developmental stage. Genetic rescue experiments and targeted manipulation of tyrosine phosphorylation further demonstrated that FGF signaling relies only partially on Frs2 and Shp2 for Grb2 recruitment, ultimately activating Ras and preventing cell death. Contrary to prevailing expectations, while both the adaptor function and the phosphatase activity of Shp2 are vital for embryonic survival, they play a surprisingly modest role in lens development, challenging the current understanding of Shp2 signaling mechanism. Notably, our research suggests that Shc may provide an alternative pathway for Grb2 recruitment and subsequent Ras activation. Although various adaptor proteins like Frs2, Crk, Shb, and Gab have been recognized for their roles in FGF signal transduction, recent findings suggest that mutations in their binding sites on FGF receptors have a significantly lesser impact compared to *Fgfr* null mutations (Brewer *et al.*, 2015; Klint and Claesson-Welsh, 1999). Our data propose that Shc1 serves as an alternative route for FGF signal transmission, thereby adding a new dimension to our understanding of FGF signaling dynamics.

Lens induction, the pivotal event in eye development, has captivated developmental biologists since Hans Spemann's seminal discovery over a century ago, which identified the optic vesicle's role in triggering the overlying head ectoderm to differentiate into the lens (Spemann,

1901). However, the nature of the lens inductive signal has remained elusive (Makrides et al., 2022; Robinson, 2006). Previous studies suggested that FGF signaling might not be essential, as deleting Fgfr1/2 in the head ectoderm did not affect the expression of the early lens determination gene, Foxe3 (Garcia *et al.*, 2011). Contrary to this notion, we have ablated all FGFRs present in the surface ectoderm, which led to a complete loss of pERK, confirming the absence of FGF signaling activity. Although the mutant ectoderm still expressed Pax6, it failed to upregulate Sox2 and Foxe3, the definitive markers of the lens induction. Moreover, the disruption of FGF signaling prevented the apical confinement of F-actin, impeding lens placode invagination driven by apical constriction (Chauhan *et al.*, 2011). Considering the concomitant expression of FGF ligands in the optic vesicle, our findings suggest that FGF signaling is an indispensable factor in lens induction.

The role of Shp2 phosphatase in enhancing Receptor Tyrosine Kinase (RTK) signaling pathways is well established, yet its molecular mechanism remains largely resolved (Neel et al., 2003). The prevailing model posits that Shp2 functions by dephosphorylating key tyrosine residues on target proteins, thereby activating Ras signaling. However, it has also been suggested that Shp2 itself can undergo C-terminal phosphorylation, potentially serving as a docking platform for other signaling molecules. Through targeted mutagenesis of these putative phosphorylation sites ($Shp2^{YF}$), we demonstrate the critical role of Shp2 phosphorylation in placental formation and neonatal survival. Biochemical analyses revealed distinct cellular responses to FGF and PDGF stimulation in $Shp2^{YF}$ mutants, suggesting context-dependent functions for these C-terminal modifications, which may explain the narrow phenotypic spectrum associated with the $Shp2^{YF}$ mutation. Intriguingly, the inactivation of Shp2 phosphatase activity via the $Shp2^{CS}$ mutation also resulted in minimal disruption of FGF signaling in lens

development, unlike the control *Le-Cre; Shp2*$^{f/f}$ mutant, which showed a significant reduction in pERK levels and subsequent lens differentiation defects. This lack of a robust phenotype cannot be attributed to residual protein activity following Cre-mediated gene deletion due to the systemic nature of the *Shp2*^{CS} mutation. While Shp2 phosphatase deficiency did cause early embryonic lethality and abrogated the development of the more FGF-sensitive lacrimal gland, the absence of a pronounced lens phenotype calls into question the essentiality of Shp2 phosphatase activity for its overall function. Given the distinct phenotype observed in the *Shp2*^{YF} mutant, it is plausible that Shp2 fulfills dual roles as both an adaptor and a phosphatase in certain signaling contexts, challenging existing paradigms and inviting further investigation into its multifaceted biological functions.

Previous studies have identified FGFR as a docking station for various signaling adaptor proteins, including Frs2, Plcg, Crk, Grb14 and Shb. In a heroic effort, Soriano and colleagues have eliminated these binding sites, both individually and collectively, but the outcomes were unexpectedly mild compared to the more severe phenotypes observed in the corresponding null mutants (Brewer *et al.*, 2015; Clark and Soriano, 2024). For instance, whereas the *Fgfr1* null mutant is lethal by E6.5, mutants lacking the ability to bind Frs2, CrkL and Plcg/Shb/Shc/Grb14 survive until E10.5. More strikingly, *Fgfr2* null mutants typically succumb by E10.5 due to widespread organ development failures, yet mutants deficient in these specific binding sites can reach adulthood with minimal apparent defects. The fact that combining *Fgfr1/2* signaling mutations does not mimic the null phenotype further suggests that these mild mutant phenotypes are not simply a result of compensatory actions by other FGF receptors. This discrepancy highlights a crucial gap in our understanding of FGF signaling, implying the existence of unidentified factors that can compensate for the loss of Frs2 and other adaptors. Our study

proposes Shc1 as a potential player in this complex signaling web, which is consistent with the observations that Shc1 can be phosphorylated in association with FGF receptors at sites known to facilitate Grb2 binding (Klint et al., 1995; Schuller et al., 2008), indicating an alternative route for signal propagation. Although *Shc1* knockout models exhibit relatively mild lens phenotypes, which may be attributed to the redundancy among Shc family proteins and potential compensation by Frs2, simultaneous deletion of *Shc1*, *Frs2* and *Shp2* further worsened lens development defects. These findings point towards a robust and adaptable FGF signaling network, capable of engaging alternative pathways through Frs2, Shc, and other adaptor proteins, thereby maintaining its function despite significant genetic disruptions. These insights underscore the complexity and resilience of cellular signaling networks, understanding which is important for developing strategies to manipulate them in developmental and disease contexts.

Methods and Materials

Mice

All procedures related to animal care and experimentation were conducted in adherence to the protocols and guidelines approved by the Institutional Animal Care and Use Committee at Columbia University. We obtained $Fgfr1^{\Delta Frs}$ from Dr. Raj Ladher (RIKEN Kobe Institute-Center for Developmental Biology, Kobe, Japan) (Hoch and Soriano, 2006), $Fgfr2^{LR}$ from Dr. Jacob V.P. Eswarakumara (Yale University School of Medicine, New Haven, CT) (Eswarakumar *et al.*, 2006) and $Fgfr2^{flox}$ from Dr. David Ornitz (Washington University Medical School, St Louis, MO) (Yu et al., 2003). $Fgfr3^{flox}$ from Dr. Xin Sun (University of California San Diego, La Jolla, CA) (Su et al., 2010), $Fgfr4^{-/-}$ from Dr. Chu-Xia Deng (National Institute of Health, Bethesda,

MD) (Weinstein et al., 1998), *Frs2α*^{flox} from Fen Wang (Texas A&M, Houston, TX) (Lin et al., 2007), *Grb2*^{flox} from Dr. Lars Nitschke (University of Erlangen-Nürnberg, Erlangen, Germany) (Ackermann et al., 2011), *Le-Cre* from Richard Lang (Children's Hospital Research Foundation, Cincinnati, OH) (Ashery-Padan *et al.*, 2000), P6 5.0 *lacZ* (*Pax6-LacZ*) reporter transgenic mice from Dr. Paul A. Overbeek (Baylor College of Medicine, Houston, TX) (Makarenkova et al., 2000), *Shc1*^{flox} from Tony Pawson (University of Toronto, Ontario, Canada) (Hardy et al., 2007), *Shp2*^{flox} from Gen-sheng Feng (UCSD, Sad Diego, CA) (Zhang et al., 2004), *LSL-Kras*^{G12D} mice was obtained from the Mouse Models of Human Cancers Consortium (MMHCC) Repository at National Cancer Institute (Tuveson *et al.*, 2004). *Bax*$^{flox/flox}$*;Bak*$^{KO/KO}$ (Stock No: 006329), *Fgfr1*^{flox} (Stock No: 007671), *Sox2Cre* (Stock No: 008454) mice were obtained from Jackson Laboratory. Animals were maintained on mixed genetic backgrounds. In all conditional knockout experiments, mice were maintained on a mixed genetic background and *Le-Cre* only or *Le-Cre* and heterozygous flox mice were used as controls. Mouse maintenance and experimentation were performed according to protocols approved by Columbia University Institutional Animal Care and Use Committee.

Shp2^{YF}, *Shp2*^{CS} and *Grb2*^{YF} targeting vectors were constructed using the recombineering method from C57BL/6 Bac clones (RP23-257E17 for *Shp2*, P23-2814 for *Grb2*, BACPAC Resources Center at Children's Hospital Oakland Research Institute) (Carbe et al., 2012). The *Shp2*^{YF} vector includes a neomycin resistance (*Neo*) cassette bordered by *loxP* sites, along with exon 14 of the *Shp2* gene harboring Y542F mutations and exon 15 with Y580F mutations. The *Shp2*^{CS} vector comprises a *NeoSTOP* cassette encased by *loxP* sites and exon 11 of the *Shp2* gene with the C483S mutation. Similarly, the *Grb2*^{YF} vector contains a *NeoSTOP* cassette flanked by *loxP* sites and exon 3 of the *Grb2* gene with the Y209F mutation. These targeting constructs,

once linearized, were introduced into C57BL/6 and 129 hybrid ES cells via electroporation. *Shp2*^{YF} recombinant clones were screened by Southern blot analysis with 5' and 3' external probes after restriction digestion with *EvoR V*, while *Grb2*^{YF} and *Shp2*^{CS} clones were identified by long-range PCR before being injected into C57BL/6 blastocysts. Chimeras were further bred with C57BL/6 mice for germline transmission, verified through PCR genotyping with specific primers for each mutation: *Grb2*^{YF} *F*: 5'- TGGGGGTCAAAGTCAAAGAG -3'; *R*: 5'- CGGAGGGAGTGAGGTATGAG -3' (wild type: 179 bp, mutant: 270 bp), *Shp2*^{YF} *F*: 5'- AAAAAGAGGCTGCTCTGCAC -3'; *R*: 5'- TCTGCAGAATGAGGGAGGAC -3' (wild type: 195 bp, mutant: 250 bp) and *Shp2*^{YF} *F*: 5'- TGGGAAGACAGACTGCAGTC-3'; *R*: 5'- GAAGGAGCACCTGCCTGTTA-3' (wild type: 180 bp, mutant: 210 bp). The Neo cassette was subsequently excised by breeding with an *EIIa-cre* transgenic line (stock number 003724, Jackson Laboratory, Bar Harbor, ME).

Database Analysis

The cumulative references for each phosphorylation site, derived from both low-throughput (LTP) and high-throughput (HTP) experiments, were sourced from the PhosphositePlus database (phosphosite.org) and graphically represented along the amino acid sequence. The expression data for lens genes from embryonic days 10.5 to 12.5 was extracted from the iSyTE database (https://research.bioinformatics.udel.edu/iSyTE/ppi/expression.php) and visualized as heatmaps to illustrate the variations in expression levels over time.

Histology and immunohistochemistry

Histology and immunohistochemistry were performed on the paraffin and cryosections as previously described (Carbe *et al.*, 2012; Carbe and Zhang, 2011). For hematoxylin and eosin

(H&E) staining, 10 µM paraffin sections underwent deparaffinization with histosol wash, rehydration through decreasing concentrations of ethanol solutions, and final washing in water. The slides were immersed in hematoxylin for 3 minutes, followed by a 10-15 minute wash with tap water. Subsequently, they were decolorized with 1% acid alcohol for 30 seconds before treatment with eosin for 1 minute. Samples were dehydrated through increasing ethanol concentrations, transferred to histosol, and mounted using a Permount mounting medium. For X-gal staining, the mouse lacrimal gland was exposed by dissecting away the periocular skin and fixed in 4% paraformaldehyde at 4 ºC overnight.

The antibodies used are phospho-ERK1/2 (#4370), phospho-mTOR (#2971), phospho-S6 (#5364), phospho-Shc (#2434), phospho-MEK1/2 (#2338), phospho-Smad1/5/9 (#13820), LEF1 (#2230), Cleaved caspase3 (#9662), cyclin D1 (#2926, discontinued), cyclin-D1 (#2978), cyclin-D3(#2936), N-cadherin (#13116) (all from Cell Signaling Technology), Fibronectin (AB2033) (from Millipore), Foxe3 (#377465), Jag1(#6011), Maf (#7866) (all from Santa Cruz), E-cadherin (#610181) and Ki67 (#550609) (both from BD Pharmingen), GFP (GFP-1010) (from Aves Labs), p57 (#75947) (from Abcam), Prox1 (PRB-238C) and Pax6 (PRB-278P) (both from Covance), Sox2 (14-9811-82) (from Thermo Fisher). Antibodies against α- and γ-crystallins were kindly provided by Sam Zigler (National Eye Institute, Bethesda, MD).
Phospho-ERK, phopho-MEK, phospho-mTOR, phosphor-Shc and phospho-Akt staining was amplified using a Tyramide Signal Amplification kit (TSATM Plus System, PerkinElmer Life Sciences, Waltham, MA). Alexa Fluor secondary antibodies and Alexa Fluor 488 phalloidin (A-12379) were ordered from Invitrogen. TUNEL staining was performed following the in situ cell

death detection kit (Roche Applied Science, Indianapolis, IN). All commercial antibodies were validated by vendors. At least three embryos of each genotype were stained for each marker.

Cell culture and western blot

Primary mouse embryonic fibroblast (MEF) cells were generated according to a previously published protocol and cultured in Dulbecco's modified Eagle's medium (DMEM) supplemented with 10% FBS and 1% penicillin-streptomycin. Adenovirus expressing Cre recombinase (Ad-cre) (Gene Transfer Vector Core, University of Iowa, IA.) were applied to MEF cells carrying flox alleles for 5 days to achieve gene deletion, while adenovirus expressing GFP (Ad-GFP) served as a control treatment. To assess growth factor responses, MEF cells were starved overnight and then treated with either FGF2 (50 ng/µl) or PDGFA (20 ng/µl) (from R&D systems) for 5 mins. Cells were immediately washed with cold PBS and harvested in ice-cold CelLytic buffer (C2978, Sigma-Aldrich, St.Louis, MO) supplemented with protease and phosphatase inhibitor cocktails (Pierce, Rockford, IL). Extracted proteins were subjected to standard western blot analysis. The antibodies used include ERK1/2 (#4695), phospho-Shp2 (#15543), phospho-Crk(#3491), phospho-Gab1(#3234), phopho-Frs2 (#3861), phospho-Shc (#2434) (all from Cell Signaling Technology), along with phospho-ERK1/2 (#7383) from Santa Cruz Biotechnology.

Quantification and Statistical Analysis

The relative lens sizes were measured using Image J and normalized against the control. The anterior/posterior lens ratio was determined by comparing the length of the anterior epithelium, as measured in Image J, to the length of the posterior lens boundary. The percentage of TUNEL and cleaved-caspase3 positive cells were normalized against the total number of DAPI positive

cells. Statistical analysis was performed using GraphPad Prism 7. Sample sizes were not predetermined. Data represent mean ± s.d. Statistical differences between two groups were assessed using an unpaired, two-tailed t-test, while comparisons among three or more groups employed one-way ANOVA followed by Tukey's multiple comparison test.

Acknowledgements

The authors thank Drs. Ruth Ashery-Padan, Chu-Xia Deng, Jacob V.P. Eswarakumara, Gensheng Feng, Raj Ladher, Richard Lang, Lars Nitschke, David Ornitz, Paul A. Overbeek, Tony Pawson, Philippe Soriano, Xin Sun, Fen Wang for mice. The work was supported by grants from NIH (R01EY017061 and R01EY025933 to X.Z.). Q.W. is supported by a Pathway to Independence Award (K99EY032171). The Columbia Ophthalmology Core Facility is supported by NIH Core grant 5P30EY019007 and unrestricted funds from Research to Prevent Blindness (RPB).

References

Ackermann, J.A., Radtke, D., Maurberger, A., Winkler, T.H., and Nitschke, L. (2011). Grb2 regulates B-cell maturation, B-cell memory responses and inhibits B-cell Ca2+ signalling. EMBO J *30*, 1621-1633. 10.1038/emboj.2011.74.

Ahmed, Z., Lin, C.C., Suen, K.M., Melo, F.A., Levitt, J.A., Suhling, K., and Ladbury, J.E. (2013). Grb2 controls phosphorylation of FGFR2 by inhibiting receptor kinase and Shp2 phosphatase activity. J Cell Biol *200*, 493-504. 10.1083/jcb.201204106.

Ahmed, Z., Timsah, Z., Suen, K.M., Cook, N.P., Lee, G.R.t., Lin, C.C., Gagea, M., Marti, A.A., and Ladbury, J.E. (2015). Grb2 monomer-dimer equilibrium determines normal versus oncogenic function. Nat Commun *6*, 7354. 10.1038/ncomms8354.

Araki, T., Nawa, H., and Neel, B.G. (2003). Tyrosyl phosphorylation of Shp2 is required for normal ERK activation in response to some, but not all, growth factors. J Biol Chem *278*, 41677-41684. 10.1074/jbc.M306461200.

Ashery-Padan, R., Marquardt, T., Zhou, X., and Gruss, P. (2000). Pax6 activity in the lens primordium is required for lens formation and for correct placement of a single retina in the eye. Genes Dev *14*, 2701-2711.

Beenken, A., and Mohammadi, M. (2009). The FGF family: biology, pathophysiology and therapy. Nature reviews. Drug discovery *8*, 235-253. 10.1038/nrd2792.

Brewer, J.R., Mazot, P., and Soriano, P. (2016). Genetic insights into the mechanisms of Fgf signaling. Genes Dev *30*, 751-771. 10.1101/gad.277137.115.

Brewer, J.R., Molotkov, A., Mazot, P., Hoch, R.V., and Soriano, P. (2015). Fgfr1 regulates development through the combinatorial use of signaling proteins. Genes Dev *29*, 1863-1874. 10.1101/gad.264994.115.

Carbe, C., Hertzler-Schaefer, K., and Zhang, X. (2012). The functional role of the Meis/Prep-binding elements in Pax6 locus during pancreas and eye development. Dev Biol *363*, 320-329. 10.1016/j.ydbio.2011.12.038.

Carbe, C., and Zhang, X. (2011). Lens induction requires attenuation of ERK signaling by Nf1. Hum Mol Genet *20*, 1315-1323. ddr014 [pii]
10.1093/hmg/ddr014.

Chauhan, B.K., Lou, M., Zheng, Y., and Lang, R.A. (2011). Balanced Rac1 and RhoA activities regulate cell shape and drive invagination morphogenesis in epithelia. Proc Natl Acad Sci U S A *108*, 18289-18294. 10.1073/pnas.1108993108.

Clark, J.F., and Soriano, P. (2024). Diverse Fgfr1 signaling pathways and endocytic trafficking regulate early mesoderm development. bioRxiv. 10.1101/2024.02.16.580629.

Collins, T.N., Mao, Y., Li, H., Bouaziz, M., Hong, A., Feng, G.S., Wang, F., Quilliam, L.A., Chen, L., Park, T., et al. (2018). Crk proteins transduce FGF signaling to promote lens fiber cell elongation. Elife *7*. 10.7554/eLife.32586.

Cvekl, A., and Zhang, X. (2017). Signaling and Gene Regulatory Networks in Mammalian Lens Development. Trends Genet *33*, 677-702. 10.1016/j.tig.2017.08.001.

Dhalluin, C., Yan, K.S., Plotnikova, O., Lee, K.W., Zeng, L., Kuti, M., Mujtaba, S., Goldfarb, M.P., and Zhou, M.M. (2000). Structural basis of SNT PTB domain interactions with distinct neurotrophic receptors. Mol Cell *6*, 921-929. 10.1016/s1097-2765(05)00087-0.

Eswarakumar, V.P., Lax, I., and Schlessinger, J. (2005). Cellular signaling by fibroblast growth factor receptors. Cytokine Growth Factor Rev *16*, 139-149.
Eswarakumar, V.P., Ozcan, F., Lew, E.D., Bae, J.H., Tome, F., Booth, C.J., Adams, D.J., Lax, I., and Schlessinger, J. (2006). Attenuation of signaling pathways stimulated by pathologically activated FGF-receptor 2 mutants prevents craniosynostosis. Proc Natl Acad Sci U S A *103*, 18603-18608. 10.1073/pnas.0609157103.
Garcia, C.M., Huang, J., Madakashira, B.P., Liu, Y., Rajagopal, R., Dattilo, L., Robinson, M.L., and Beebe, D.C. (2011). The function of FGF signaling in the lens placode. Dev Biol *351*, 176-185. S0012-1606(11)00017-0 [pii]
10.1016/j.ydbio.2011.01.001.
Garg, A., Hannan, A., Wang, Q., Makrides, N., Zhong, J., Li, H., Yoon, S., Mao, Y., and Zhang, X. (2020). Etv transcription factors functionally diverge from their upstream FGF signaling in lens development. Elife *9*. 10.7554/eLife.51915.
Garg, A., and Zhang, X. (2017). Lacrimal gland development: From signaling interactions to regenerative medicine. Dev Dyn *246*, 970-980. 10.1002/dvdy.24551.
Gotoh, N., Ito, M., Yamamoto, S., Yoshino, I., Song, N., Wang, Y., Lax, I., Schlessinger, J., Shibuya, M., and Lang, R.A. (2004). Tyrosine phosphorylation sites on FRS2alpha responsible for Shp2 recruitment are critical for induction of lens and retina. Proc Natl Acad Sci U S A *101*, 17144-17149.
Hadari, Y.R., Gotoh, N., Kouhara, H., Lax, I., and Schlessinger, J. (2001). Critical role for the docking-protein FRS2 alpha in FGF receptor-mediated signal transduction pathways. Proc Natl Acad Sci U S A *98*, 8578-8583. 10.1073/pnas.161259898
161259898 [pii].
Haines, E., Minoo, P., Feng, Z., Resalatpanah, N., Nie, X.M., Campiglio, M., Alvarez, L., Cocolakis, E., Ridha, M., Di Fulvio, M., et al. (2009). Tyrosine phosphorylation of Grb2: role in prolactin/epidermal growth factor cross talk in mammary epithelial cell growth and differentiation. Mol Cell Biol *29*, 2505-2520. 10.1128/MCB.00034-09.
Hardy, W.R., Li, L., Wang, Z., Sedy, J., Fawcett, J., Frank, E., Kucera, J., and Pawson, T. (2007). Combinatorial ShcA docking interactions support diversity in tissue morphogenesis. Science *317*, 251-256. 10.1126/science.1140114.
Hayashi, S., and McMahon, A.P. (2002). Efficient recombination in diverse tissues by a tamoxifen-inducible form of Cre: a tool for temporally regulated gene activation/inactivation in the mouse. Dev Biol *244*, 305-318.
Hoch, R.V., and Soriano, P. (2006). Context-specific requirements for Fgfr1 signaling through Frs2 and Frs3 during mouse development. Development *133*, 663-673. dev.02242 [pii]
10.1242/dev.02242.
Kakrana, A., Yang, A., Anand, D., Djordjevic, D., Ramachandruni, D., Singh, A., Huang, H., Ho, J.W.K., and Lachke, S.A. (2018). iSyTE 2.0: a database for expression-based gene discovery in the eye. Nucleic Acids Res *46*, D875-D885. 10.1093/nar/gkx837.
Klint, P., and Claesson-Welsh, L. (1999). Signal transduction by fibroblast growth factor receptors. Front Biosci *4*, D165-177.
Klint, P., Kanda, S., and Claesson-Welsh, L. (1995). Shc and a novel 89-kDa component couple to the Grb2-Sos complex in fibroblast growth factor-2-stimulated cells. J Biol Chem *270*, 23337-23344. 10.1074/jbc.270.40.23337.

Kuracha, M.R., Burgess, D., Siefker, E., Cooper, J.T., Licht, J.D., Robinson, M.L., and Govindarajan, V. (2011). Spry1 and Spry2 are necessary for lens vesicle separation and corneal differentiation. Invest Ophthalmol Vis Sci *52*, 6887-6897. 10.1167/iovs.11-7531.
Li, H., Mao, Y., Bouaziz, M., Yu, H., Qu, X., Wang, F., Feng, G.S., Shawber, C., and Zhang, X. (2019). Lens differentiation is controlled by the balance between PDGF and FGF signaling. PLoS biology *17*, e3000133. 10.1371/journal.pbio.3000133.
Li, H., Tao, C., Cai, Z., Hertzler-Schaefer, K., Collins, T.N., Wang, F., Feng, G.S., Gotoh, N., and Zhang, X. (2014). Frs2alpha and Shp2 signal independently of Gab to mediate FGF signaling in lens development. Journal of cell science *127*, 571-582. 10.1242/jcs.134478.
Li, S., Couvillon, A.D., Brasher, B.B., and Van Etten, R.A. (2001). Tyrosine phosphorylation of Grb2 by Bcr/Abl and epidermal growth factor receptor: a novel regulatory mechanism for tyrosine kinase signaling. EMBO J *20*, 6793-6804. 10.1093/emboj/20.23.6793.
Lin, Y., Zhang, J., Zhang, Y., and Wang, F. (2007). Generation of an Frs2alpha conditional null allele. Genesis *45*, 554-559. 10.1002/dvg.20327.
Lovicu, F.J., and McAvoy, J.W. (2005). Growth factor regulation of lens development. Dev Biol *280*, 1-14. S0012-1606(05)00045-X [pii]
10.1016/j.ydbio.2005.01.020.
Lovicu, F.J., and Overbeek, P.A. (1998). Overlapping effects of different members of the FGF family on lens fiber differentiation in transgenic mice. Development *125*, 3365-3377.
Madakashira, B.P., Kobrinski, D.A., Hancher, A.D., Arneman, E.C., Wagner, B.D., Wang, F., Shin, H., Lovicu, F.J., Reneker, L.W., and Robinson, M.L. (2012). Frs2alpha enhances fibroblast growth factor-mediated survival and differentiation in lens development. Development *139*, 4601-4612. 10.1242/dev.081737.
Makarenkova, H.P., Ito, M., Govindarajan, V., Faber, S.C., Sun, L., McMahon, G., Overbeek, P.A., and Lang, R.A. (2000). FGF10 is an inducer and Pax6 a competence factor for lacrimal gland development. Development *127*, 2563-2572.
Makrides, N., Wang, Q., Tao, C., Schwartz, S., and Zhang, X. (2022). Jack of all trades, master of each: the diversity of fibroblast growth factor signalling in eye development. Open Biol *12*, 210265. 10.1098/rsob.210265.
Neel, B.G., Gu, H., and Pao, L. (2003). The 'Shp'ing news: SH2 domain-containing tyrosine phosphatases in cell signaling. Trends in biochemical sciences *28*, 284-293.
Ochi, H., Ogino, H., Kageyama, Y., and Yasuda, K. (2003). The stability of the lens-specific Maf protein is regulated by fibroblast growth factor (FGF)/ERK signaling in lens fiber differentiation. J Biol Chem *278*, 537-544. 10.1074/jbc.M208380200
M208380200 [pii].
Ong, S.H., Guy, G.R., Hadari, Y.R., Laks, S., Gotoh, N., Schlessinger, J., and Lax, I. (2000). FRS2 proteins recruit intracellular signaling pathways by binding to diverse targets on fibroblast growth factor and nerve growth factor receptors. Mol Cell Biol *20*, 979-989.
Pan, Y., Woodbury, A., Esko, J.D., Grobe, K., and Zhang, X. (2006). Heparan sulfate biosynthetic gene Ndst1 is required for FGF signaling in early lens development. Development *133*, 4933-4944.
Qu, X., Carbe, C., Tao, C., Powers, A., Lawrence, R., van Kuppevelt, T.H., Cardoso, W.V., Grobe, K., Esko, J.D., and Zhang, X. (2011a). Lacrimal Gland Development and Fgf10-Fgfr2b Signaling

Are Controlled by 2-O- and 6-O-sulfated Heparan Sulfate. J Biol Chem *286*, 14435-14444. M111.225003 [pii]
10.1074/jbc.M111.225003.
Qu, X., Hertzler, K., Pan, Y., Grobe, K., Robinson, M.L., and Zhang, X. (2011b). Genetic epistasis between heparan sulfate and FGF-Ras signaling controls lens development. Dev Biol *355*, 12-20. 10.1016/j.ydbio.2011.04.007.
Riera, L., Lasorsa, E., Ambrogio, C., Surrenti, N., Voena, C., and Chiarle, R. (2010). Involvement of Grb2 adaptor protein in nucleophosmin-anaplastic lymphoma kinase (NPM-ALK)-mediated signaling and anaplastic large cell lymphoma growth. J Biol Chem *285*, 26441-26450. 10.1074/jbc.M110.116327.
Robinson, M.L. (2006). An essential role for FGF receptor signaling in lens development. Semin Cell Dev Biol *17*, 726-740. 10.1016/j.semcdb.2006.10.002.
Robinson, M.L., MacMillan-Crow, L.A., Thompson, J.A., and Overbeek, P.A. (1995). Expression of a truncated FGF receptor results in defective lens development in transgenic mice. Development *121*, 3959-3967.
Schuller, A.C., Ahmed, Z., Levitt, J.A., Suen, K.M., Suhling, K., and Ladbury, J.E. (2008). Indirect recruitment of the signalling adaptor Shc to the fibroblast growth factor receptor 2 (FGFR2). Biochem J *416*, 189-199. 10.1042/BJ20080887.
Smith, A.N., Miller, L.A., Song, N., Taketo, M.M., and Lang, R.A. (2005). The duality of beta-catenin function: a requirement in lens morphogenesis and signaling suppression of lens fate in periocular ectoderm. Dev Biol *285*, 477-489.
Spemann, H. (1901). Uber Korrelationen in die Entwickelung des Auges. AVerh. Anat. Ges. *15*, 61-79.
Su, N., Xu, X., Li, C., He, Q., Zhao, L., Li, C., Chen, S., Luo, F., Yi, L., Du, X., et al. (2010). Generation of Fgfr3 conditional knockout mice. Int J Biol Sci *6*, 327-332.
Sun, J., Lu, S., Ouyang, M., Lin, L.J., Zhuo, Y., Liu, B., Chien, S., Neel, B.G., and Wang, Y. (2013). Antagonism between binding site affinity and conformational dynamics tunes alternative cis-interactions within Shp2. Nat Commun *4*, 2037. 10.1038/ncomms3037.
Tuveson, D.A., Shaw, A.T., Willis, N.A., Silver, D.P., Jackson, E.L., Chang, S., Mercer, K.L., Grochow, R., Hock, H., Crowley, D., et al. (2004). Endogenous oncogenic K-ras(G12D) stimulates proliferation and widespread neoplastic and developmental defects. Cancer Cell *5*, 375-387. S1535610804000856 [pii].
Vemulapalli, V., Chylek, L.A., Erickson, A., Pfeiffer, A., Gabriel, K.H., LaRochelle, J., Subramanian, K., Cao, R., Stegmaier, K., Mohseni, M., et al. (2021). Time-resolved phosphoproteomics reveals scaffolding and catalysis-responsive patterns of SHP2-dependent signaling. Elife *10*. 10.7554/eLife.64251.
Wang, Q., Tao, C., Hannan, A., Yoon, S., Min, X., Peregrin, J., Qu, X., Li, H., Yu, H., Zhao, J., and Zhang, X. (2021). Lacrimal gland budding requires PI3K-dependent suppression of EGF signaling. Sci Adv *7*. 10.1126/sciadv.abf1068.
Weinstein, M., Xu, X., Ohyama, K., and Deng, C.X. (1998). FGFR-3 and FGFR-4 function cooperatively to direct alveogenesis in the murine lung. Development *125*, 3615-3623.
Xie, Q., McGreal, R., Harris, R., Gao, C.Y., Liu, W., Reneker, L.W., Musil, L.S., and Cvekl, A. (2016). Regulation of c-Maf and alphaA-Crystallin in Ocular Lens by Fibroblast Growth Factor Signaling. J Biol Chem *291*, 3947-3958. 10.1074/jbc.M115.705103.

Yang, W., Klaman, L.D., Chen, B., Araki, T., Harada, H., Thomas, S.M., George, E.L., and Neel, B.G. (2006). An Shp2/SFK/Ras/Erk signaling pathway controls trophoblast stem cell survival. Dev Cell *10*, 317-327.
Yu, K., Xu, J., Liu, Z., Sosic, D., Shao, J., Olson, E.N., Towler, D.A., and Ornitz, D.M. (2003). Conditional inactivation of FGF receptor 2 reveals an essential role for FGF signaling in the regulation of osteoblast function and bone growth. Development *130*, 3063-3074.
Zhang, E.E., Chapeau, E., Hagihara, K., and Feng, G.S. (2004). Neuronal Shp2 tyrosine phosphatase controls energy balance and metabolism. Proc Natl Acad Sci U S A *101*, 16064-16069.
Zhao, H., Yang, T., Madakashira, B.P., Thiels, C.A., Bechtle, C.A., Garcia, C.M., Zhang, H., Yu, K., Ornitz, D.M., Beebe, D.C., and Robinson, M.L. (2008). Fibroblast growth factor receptor signaling is essential for lens fiber cell differentiation. Dev Biol *318*, 276-288. S0012-1606(08)00232-7 [pii]
10.1016/j.ydbio.2008.03.028.

FIGURE LEGENDS

Figure 1. FGF Signaling Regulates Lens Development in a Dose-Dependent Manner. (A) Schematic diagram of murine lens development. The head ectoderm is induced by the underlying optic vesicle to become the lens placode, which subsequently folds inwards to become the lens pit. The closure of the lens vesicle sets the stage for the differentiation of the lens epithelium into the lens fibers. **(B)** Depletion of all four *Fgfr1/2/3/4*, driven by *Le-Cre* and traced with GFP, led to a thinner lens placode, evident from the absence of pERK signals and the failure to upregulate Sox2 like Pax6 (inserts, arrowheads). **(C)** *Fgfr1/2/3/4* mutants displayed disrupted apical constriction (F-actin accumulation, arrows) and lacked lens-specific expression of Foxe3 and Jag1 (arrowheads). Dotted lines outline the lens pit. **(D)** Despite *Fgfr1/2/3/4* mutations, BMP (pSmad1/5/9 staining, arrowheads) and Wnt signaling (Lef1 expression, arrows) remained unaffected. **(E)** The absence of *Fgfr1/2* alone did not impede the apical buildup of F-actin nor the expression of Foxe3, indicating partial retention of lens development processes. **(F)** Crucial lens markers, Prox1 and αA-crystallin, were absent in *Fgfr1/2* mutants, pointing to a significant developmental defect after the lens induction stage. **(G)** *Fgfr1/2* mutants exhibited loss of cell proliferation marker Cyclin D1 (arrows) and widespread apoptosis (TUNEL staining, arrowheads).

Figure 2. Restoration of Lens Development in FGF Signaling Mutants via Kras Activation and Apoptosis Inhibition. (A) The *Le-Cre* driver facilitated the excision of the floxed alleles of *Fgf1/2* along with the *LSL-STOP* cassette at the *Kras* locus, leading to the expression of the constitutively active $Kras^{G12D}$ allele within the *Fgf1/2* mutant background. **(B)** The activation of Kras signaling in the FGF signaling mutant lenses reinstated pERK activity at E10.5 and pMEK expression at E13.5, indicating restoration of MAPK signaling. **(C)** The lens-specific expression

of Prox1 and αA-crystallin were also recovered, indicating successful lens development rescue. **(D)** Quantification of the lens size. One way ANOVA, n=3, *P<0.001, **P<0.02. **(E)** The deletion of pro-apoptotic genes *Bak* and *Bax* in *Fgf1/2* mutants suppressed apoptosis as shown by TUNEL staining. **(F)** Inhibiting apoptosis in *Fgfr1/2* mutants facilitated lens formation, as indicated by the expression of lens differentiation markers Prox1, Maf, and Jag1. **(G)** Quantification cell apoptosis. One-way ANOVA, n=3, *P<0.001. **(I)** Quantification of the lens size. One-way ANOVA, n=3, *P<0.0001, **P<0.05.

Figure 3. The Frs2 binding site on FGFR is only required for lens vesicle differentiation. **(A)** Overview of *Fgfr* mutant alleles. *Fgfr1*$^{\Delta Frs}$ lacks the Frs2 binding domain (amino acid 407-433), and *Fgfr2*^{LR} has point mutations disrupting Frs2 binding (L424A and L426A). **(B)** In *Fgf1/2* compound mutants, loss of pERK , CyclinD1, αA-crystallin and increased cleaved caspase3 were observed with the *Fgfr1*$^{\Delta Frs}$ allele but not the *Fgfr2*^{LR} allele. **(C)** Quantification of cleaved caspase3 staining. Student's t-test, n=3, *P<0.001. **(D)** Heatmap depicts *Fgfr* expression levels during lens development. **(E)** *Fgfr2*^{LR} mutants in the *Fgfr1/2/3* genetic background showed impaired lens vesicle differentiation, with posterior lens epithelial cells failing to elongate and activate lens fiber cell markers Jag1 and Maf. **(F)** *Fgfr1/2/3* triple mutants with *Fgfr2*^{LR} lost pERK staining and displayed a shallow lens vesicle at E12.5. **(G)** Quantification of the lens size. One-way ANOVA n=3, *P<0.001, **P<0.05.

Figure 4. Grb2 is essential for lens vesicle survival, proliferation, and differentiation. (A) The targeted removal of Grb2 in the lens led to a loss of pERK signaling, reduced CyclinD3 expression, increased apoptosis (TUNEL staining), and disrupted expression of critical lens development genes Maf, Foxe3, Jag1 and γ-crystallin expression at E12.5. **(B)** Grb2 mutants Grb2 mutants displayed absent CyclinD1, Prox1, and p57 expression at E11.5 and remained an

undifferentiated hollow vesicle at E13.5, failing to undergo normal lens fiber elongation. **(C)** Quantification of the lens size. Student's t-test, n=3, *P<0.0001.

Figure 5. Shp2 C-terminal tyrosine phosphorylation is required for embryonic survival but dispensable for lens development. (A) Schematic of the core FGF signaling pathway. FGFR activation leads to phosphorylation of the adaptor Frs2 on N- and C-terminal tyrosines, recruiting Grb2 and Shp2 respectively. Shp2 can also bind Grb2 via its own C-terminal phosphotyrosines, and dephosphorylates Grb2 via its catalytic cysteine residue. **(B)** Generation of the *Shp2*^{YF} allele by homologous recombination to introduce *loxP*-flanked Neo and point mutations (Y542F and Y580F) disrupting the Shp2 C-terminal phosphotyrosine sites. The Neo cassette was subsequently excised by Cre-mediated recombination. **(C)** Validation of the *Shp2*^{YF} allele targeting was confirmed through Southern blot analysis with both 5' and 3' probes. **(D)** Kaplan-Meier survival curves demonstrate early lethality of *Shp2*^{YF} embryos (E12.5) and perinatal lethality of *Sox2Cre;Shp2*$^{f/YF}$ mutants. n=5 for *Shp2*$^{YF/YF}$ and n=6 for *Sox2Cre;Shp2*$^{f/YF}$ mutants. **(E)** *Shp2*$^{YF/YF}$ embryos displayed reduced body size at E12.5 and thinner labyrinth zones in their placenta E10.5. **(F)** *Sox2Cre*-mediated targeting restricts Shp2 deficiency to the embryonic proper, circumventing placental abnormalities. **(G)** *Sox2Cre;Shp2*$^{f/YF}$ mutants appeared grossly normal at E15.5 but failed to survive after birth. **(H)** While Y542 phosphorylation in Shp2 was lost as expected, *Sox2Cre;Shp2*$^{f/YF}$ MEFs exhibited a more pronounced reduction in pERK response to PDGF stimulation compared to FGF stimulation. **(I)** *Sox2Cre;Shp2*$^{f/YF}$ mutant lens displayed normal pERK staining and morphology, but reduced pERK in lacrimal glands at E14.5 and decreased bud numbers at P0. **(J)** Quantification of the number of lacrimal gland buds. Student's t-test, n=3, *P<0.02.

Figure 6. Shp2 phosphatase activity is partially required for FGF signaling independently of Grb2 dephosphorylation. (A) PhosphositePlus database indicates that Grb2 predominantly undergoes phosphorylation at Y209 and less frequently at Y160. **(B)** The *Grb2*^{YF} allele was constructed by homologous recombination to integrate a *loxP*-flanked *Neo* cassette and a Y209F point mutation into the *Grb2* locus. **(C)** PCR genotyping confirmed the presence of the *Grb2*^{YF} allele. **(D)** *Grb2* mutant lens typical expression patterns of pERK, cell cycle markers p57 and Ki67 and differentiation markers Foxe3, Maf and Jag1. **(E)** The *Shp2*^{CS} allele was generated by inserting the C459S mutation into the Shp2 locus by homologous recombination, followed by Cre-mediated removal of the *loxP*-flanked *Neo* cassette. **(F)** *Shp2*^{CS} allele validated by PCR genotyping. **(G)** *Shp2*$^{CS/CS}$ mutants exhibited growth retardation and died at E9.5. **(H)** *Shp2*$^{f/CS}$ MEF cells retained a significant capacity to activate pERK upon FGF stimulation after Cre virus infection. **(I)** *Le-Cre;Shp2*$^{f/f}$ mutants exhibited loss of pERK and Jag1 staining at the lens transition zone (arrowheads), which also shifted posteriorly. *Le-Cre;Shp2*$^{f/CS}$ mutant lens, in contrast, maintained staining at the equatorial region. Notably, both mutant types lacked lacrimal gland buds (arrows). **(J)** Quantification of the lens size. One-way ANOVA n=3, *P<0.0001, **P<0.001. **(K)** Quantification of the lens perimeter spanning the anterior epithelium versus that of the posterior lens fiber. One-way ANOVA n=3, *P<0.001.

Figure 7. Shc1 complements Frs2 and Shp2 in mediating FGF signaling in lens development. (A) *Fgfr1*$^{f/f}$*;Fgfr2*$^{f/LR}$ infected with Cre virus showed stronger pERK and pShc activation than *Fgfr1*$^{f/\Delta Frs}$*;Fgfr2*$^{f/f}$ MEF cells, despite both losing Frs2, Shp2, Gab1, and Crk phosphorylation. **(B)** pShc staining was lost in *Le-Cre;Fgfr1*$^{f/\Delta Frs}$*;Fgfr2*$^{f/f}$ mutant lens (arrowhead) but preserved in *Le-Cre;Fgfr1*$^{f/f}$*;Fgfr2*$^{f/LR}$ lens. **(C)** Heatmap showing Shc expression levels during lens development. **(D)** *Shc1*-deficient lenses showed a slight decrease in

both pERK staining intensity and overall lens size. **(E)** E12.5 Frs2/Shc1 mutant lenses were smaller than controls, while lenses from Frs2/Shp2 mutants showed a pronounced hollow vesicle structure, a condition that worsened in Frs2/Shp2/Shc1 triple mutants. **(F)** Quantification of the lens size. One-way ANOVA n=4, *P<0.001, **P<0.05. **(G)** Model of FGF signaling network. Frs2 recruits Grb2 directly and indirectly through Shp2, while Shc1 provides an alternate Grb2 recruitment route independent of Frs2.

Supplementary Figure 1. Lens development in Fgf receptor mutants. (A) Depletion of all four *Fgfr1/2/3/4* did not disrupt the Fibronectin expression at the basal side of the lens placode (arrows). **(B)** pmTOR and pS6 staining were lost in *Le-Cre;Fgfr1*$^{f/f}$*;Fgfr2*$^{f/LR}$ lens.

Supplementary Figure 2. Cell proliferation and apoptosis in *Shp2*^{CS} mutants. *Le-Cre;Shp2*$^{f/CS}$ lens exhibits normal expression of proliferation marker Ki67, but there is a significant increase in TUNLE+ cells (arrowheads). Student's t-test, N.S. (not significant) for %Ki67+ cells and P<0.01 for %TUNEL+ cells in the lens epithelium.